THINK SMARTER NOT HARDER: ADAPTIVE REASONING WITH INFERENCE AWARE OPTIMIZATION

Zishun Yu*
Department of Computer Science
The University of Illinois Chicago
Chicago, IL 60607, USA
zyu32@uic.edu

Tengyu Xu, Di Jin, Karthik Abinav Sankararaman,
Yun He, Wenxuan Zhou, Zhouhao Zeng, Eryk Helenowski,
Chen Zhu, Sinong Wang, Hao Ma & Han Fang
Meta AI
Menlo Park, CA 94025, USA

ABSTRACT

Solving mathematics problems has been an intriguing capability of language models, and many efforts have been made to improve reasoning by extending reasoning length, such as through self-correction and extensive long chain-of-thoughts. While promising in problem-solving, advanced long reasoning chain models exhibit an undesired uni-modal behavior, where trivial questions require unnecessarily tedious long chains of thought. In this work, we propose a way to allow models to be aware of inference budgets by formulating it as utility maximization with respect to an inference budget constraint, hence naming our algorithm Inference Budget-Constrained Policy Optimization (IBPO). In a nutshell, models fine-tuned through IBPO learn to "understand" the difficulty of queries and allocate inference budgets to harder ones. With different inference budgets, our best models are able to have a 4.14% and 5.74% absolute improvement (8.08% and 11.2% relative) on MATH500 using 2.16x and 4.32x inference budgets respectively, relative to LLaMA3.1 8B Instruct. These improvements are approximately 2x those of self-consistency under the same budgets.

1 INTRODUCTION

Complex reasoning has been an intriguing ability of large language models (LLMs), with application in for example mathematical problem-solving (Cobbe et al., 2021; Hendrycks et al., 2021b; Lightman et al., 2023) or coding (Chen et al., 2021; Austin et al., 2021; Hendrycks et al., 2021a), which does not only require nature language comprehending but also logical and critical "thinking". An observation merged in the LLM reasoning literature is that longer reasoning traces often leads to improved reasoning soundness and correctness. The seminal work of chain-of-thought (CoT) (Wei et al., 2022) is an excellent example of how enriching reasoning details, by decomposing reasoning traces into steps, improves its problem-solving capability. CoT has been considered a standard technique in reasoning, recent works extend CoT by allow LLMs to expand its reasoning steps, by for example CoT with more steps (Jin et al., 2024) (as explicitly required by instruction), self-reflection/correction (Madaan et al., 2024; Zelikman et al., 2022; Yan et al., 2024; Qu et al., 2024), multi-turn reasoning (Kumar et al., 2024) or multi-agent debate (Liang et al., 2023; Pham et al., 2023) (as a heterogeneous case of multi-turn). It was conjectured that scaling the test-time compute or the reasoning length unleashes LLMs' potential for reasoning (Snell et al., 2024), which has been empirically verified by recent hype of ultra-long reasoning models, such as OpenAI-o1 (Jaech et al., 2024) and DeepSeek-R1 (DeepSeek-AI et al., 2025). We'll later categorizes these type of responses as (standard) CoT responses, extended responses, and (ultra-)long responses, respectively.

While scaling reasoning length is promising, advanced long reasoning-chain models show an undesired uni-modal behavior that trivial questions may require unnecessarily tedious long reasoning trace, an example is shown in Appendix A. This uni-modal behavior creates unnecessarily higher inference costs and increased carbon footprints (Henderson et al., 2020; Anthony et al., 2020). To partially address this, we study how to enable multi-modal behavior for reasoning models in a way the length of reasoning traces are automatically adjusted according to the hardness level of the queries.

*Work done at Meta.

From the aspect of query-adaptive reasoning length, some heuristic methods (e.g. Aggarwal et al., 2023; Xu et al., 2024a; Wang et al., 2024) have been making effort towards better token efficiency, by which is meant better accuracy with (hopefully) less token overhead. We take a reinforcement learning (RL) perspective, where the accuracy gain over the token overhead is nothing but a non-differentiable objective to be optimized. One could, for instance, take the negative response length or a metric of this sort as an intrinsic reward (Chentanez et al., 2004; Pathak et al., 2017). However, balancing the intrinsic and extrinsic (accuracy) rewards can be challenging (Liu et al., 2021), and be vulnerable to reward hacking (Pan et al., 2022; Skalse et al., 2022; Karwowski et al., 2023).

Instead explicit modeling the length of responses, we take a more abstract formulation, where we consider labeling each response y with an unique group label $\mathcal{G}_i : i \in [\![G]\!]$ for total number of G groups, so that the union of these disjoint groups exactly form the response space $\cup_i \mathcal{G}_i = \mathcal{Y}$. For example $\mathcal{G}$ could be the group of CoT responses (with standard length) or extended responses. We could then impose an density constraint on each or a set of groups, by caping $\mathbb{E}_{x\sim\mu}\mathbb{E}_{y\sim\pi(x)}[\mathbb{1}_{\{y\in\mathcal{G}_i\}}] \leq q_i$ for some prompt distribution μ and some response distribution $\pi(x)$, induced from LLMs, conditioned on a prompt x. This naturally formulates a constrained RL (Garcıa & Fernández, 2015; Altman, 2021) problem. Also this group definition is motivated by the resource-allocation literature (Chenery & Kretschmer, 1956; Ibaraki & Katoh, 1988; Karlin, 2003), from the optimization and econometric communities, which have been later applied in many machine learning applications (e.g. Zemel et al., 2013; Badanidiyuru et al., 2018). This generalization allows potential broader application of our algorithm as discussed in Section 6. We've now set our goal:

> A constrained RL framework controlling how response groups $\{\mathcal{G}_i\}$ are distributed.

Therefore, one could control how responses of different lengths (which are supposed to belong to different groups) are distributed. Our rationale of algorithm design is given in Section 2, derived from an optimization perspective but ended as a very simple generalization of iterative supervised fine-tuning (SFT) methods such as reward-ranking fine-tuning (RAFT) (Dong et al., 2023) and rejection sampling fine-tuning (RFT) (Ouyang et al., 2022; Touvron et al., 2023), see details in Section 3. Given the motivation of our algorithm, we call the resulted algorithm as Inference Budget-Constrained Policy Optimization (IBPO).

Paper structure. Section 2 present the derivation of our algorithm from an optimization view, resulting in a simple weighted iterative SFT update. Section 3 provides further details on practical implementation, including the base algorithm and the reward design. Section 4 introduces some experimental settings. The empirical results of our IBPO are presented in Section 5. And Section 6 concludes our work with limitations, broader impact, and further discussions.

2 Algorithm Design

Problem setup. To make the notation compact, we take the bandit notation (or the sequence-level notation), commonly used in LLMs (Ziegler et al., 2019; Rafailov et al., 2024), especially in preference modeling, that suppresses the transition probabilities and the token-level rewards, and see a response as a whole. In particular, a policy $\pi : \mathcal{X} \to \Delta(\mathcal{Y})$ takes a prompt $x \in \mathcal{X}$ and draw a response $a_1 \circ a_2 \cdots \circ a_T =: y \in \mathcal{Y}$ from the produced probability simplex $\Delta(\mathcal{Y})$, where $\circ$ denotes concatenation, $a_i \in \mathcal{V}$ corresponds to the i-th token drawn from the vocabulary $\mathcal{V}$, and T is the maximum length. A LLM is a parametric policy $\pi_\theta \in \Pi_\theta \subseteq \Pi$, where Π_θ and Π are the parametric and non-parametric policy space respectively. Let $\mathcal{J}(\pi; \mu, r)$ or sometimes $\mathcal{J}(\pi)$ be a general objective, defined by a bounded reward function $r : \mathcal{X} \times \mathcal{Y} \to [-R_{\max}, R_{\max}]$, and a prompt distribution $\mu \in \Delta(\mathcal{X})$. Also, we define μ_Ω as an empirical distribution induced from Ω, a set of prompts.

As aforementioned, we define G disjoint groups $\mathcal{G}_i$ such that $\cup_i \mathcal{G}_i = \mathcal{Y}$ and $\mathcal{G}_i \cap \mathcal{G}_j = \emptyset$ for all $i \neq j$. Each response $y \in \mathcal{Y}$ is attached to exactly one group, in the sense that $y \in \mathcal{G}_i$ for some i. In the context of LLM reasoning, without loss of generality, we consider two groups for brevity: $\mathcal{G}_\circ$ and $\mathcal{G}_+$, corresponding to regular-length CoT responses and extended responses (with low and high inference costs), respectively. To conclude the formulation of constrained RL with resource allocation constraints, we could in general define the feasible set as a convex polytope, $\Phi_\mathcal{G} := \{\pi : \mathbb{E}_x\mathbb{E}_{y\sim\pi(x)}[\mathbb{1}_{\{y\in\mathcal{G}_i\}}] \leq q_i \text{ for all } i\}$, that caps the total density mass of each group

$\mathcal{G}_i$ by q_i. In our setting, we only need to cap the total mass of extended responses to optimize the inference efficiency, posing a half-space $\Phi_+ := \{\pi : \mathbb{E}_x \mathbb{E}_{y\sim\pi(x)}[\mathbb{1}_{\{y\in\mathcal{G}_+\}}] \leq q_+\}$ for some $q_+ > 0$.

Background. With the bandit setup, our setting draw a lot connections to the online learning literature, especially online/bandit convex optimization (Hazan et al., 2016; Slivkins et al., 2019), although we optimize a fixed function the training data is however collected in an online fashion. In the sense of distributing resources across groups, it is connected to for example knapsack bandits (Badanidiyuru et al., 2018) and statistical parity (Zemel et al., 2013), aka group fairness. Although the definition of groups and optimization programs could be different. This allocation optimization point of view allows us to further extend our method to broader LLM applications. To the end of policy optimization with constraints, common techniques include projection (Zinkevich, 2003; Flaxman et al., 2004; Bubeck et al., 2015; Yang et al., 2020), Lyapunov-based (Chow et al., 2018; Cayci et al., 2022), or Lagrangian methods (Ray et al., 2019).

Non-parametric space Π. In our case, our goal is to solve:

$$\max_{\pi_\theta\in\Pi_\theta} \mathcal{J}(\pi_\theta) \quad \text{s.t. } \pi_\theta \in \Phi_+ \tag{1}$$

where Π_θ is the parameterized policy space. Solving (1) is however intractable due to the LLM parameterized policy space Π_θ. A common practice is alternating gradients between reward maximization and constraint satisfaction. For example in Lagrangian methods such as TRPO/PPO-Lagrangian (Ray et al., 2019), one could do alternating update π_θ and the Lagrangian multiplier. Another workaround is to first obtain a solution $\pi^\star$ in the non-parametric policy space $\Pi := \Delta(\mathcal{X}\times\mathcal{Y})$, aka tabular representations, and project $\pi^\star$ onto the parameteric one Π_θ, as a technique used in many (constrained) RL works (Peters et al., 2010; Montgomery & Levine, 2016; Zhang et al., 2020).

The advantage of working in the non-parametric space Π is: solving $\max_{\pi\in\Pi} \mathcal{J}(\pi)$ s.t. $\pi \in \Phi_+$ is easy, on the conditions that (i) $\mathcal{J}(\pi)$ is concave in π so that it is a convex program, and (ii) sampling and evaluating the reward function $r(\cdot,\cdot)$ and the cost indicator $\mathbb{1}_{\{\cdot\}}$ are cheap. The condition (i) is sometimes true, for instances: bandit objective (Slivkins et al., 2019); the LP formulation (Manne, 1960; Denardo, 1970; Nachum & Dai, 2020; Nachum et al., 2019), and (relative) entropy regularized RL (Ziebart, 2010; Haarnoja et al., 2017; 2018) objectives are concave in occupancy measure ρ. However, in rare case condition (ii) holds, RL works (Haarnoja et al., 2018; Peng et al., 2019; Zhang et al., 2020) often resort to value function approximation, making it is easy, for discrete action space, to evaluate Q-values (or alternatively advantages) for all actions for a specific state. It is then tractable to obtain closed-form solution (optimal w.r.t. the value/advantage approximations) in Π. Once an optimal policy $\pi^\star$ is found, one could then project it onto Π_θ through (reverse) information projection $\theta = \arg\min_\theta \mathbb{KL}(\pi^\star\|\pi_\theta)$ (often done approximately by taking gradient steps).

Stochastic optimization. With a LLM, it is obviously intractable to sample and evaluate the reward function $r(x,y)$ for all $(x,y)\in\mathcal{X}\times\mathcal{Y}$, similarly for the cost indicator $\mathbb{1}_{\{\cdot\}}$. To avoid the training of additional value models for LLMs (Snell et al., 2022; Yu et al., 2023), which can create significant overhead in terms of memory usage, implementation complexity, and training stability, we consider a stochastic optimization. The stochastic counterpart as described in (2) solves an approximate $\hat{\pi}^\star$ using a manageable number of samples rather than directly solving the optimum $\pi^\star$, still, in Π:

$$\begin{aligned} \hat{\pi}^\star(\mathbf{X},\mathbf{Y}) \in \arg\max_{\pi\in\Pi} \hat{\mathcal{J}}(\pi;\mathbf{X},\mathbf{Y}) &:= \tfrac{1}{nm}\textstyle\sum_i^n \sum_j^m [\pi(y_{ij}|x_i) r(x_i,y_{ij})] \\ \text{s.t. } \pi \in \hat{\Phi}_+(\mathbf{X},\mathbf{Y}) &:= \{\pi : \textstyle\sum_i\sum_j [\pi(y_{ij}|x_i)\big(\mathbb{1}_{\{y_{ij}\in\mathcal{G}_+\}} - q_+\big)] \leq 0\} \end{aligned} \tag{2}$$

where $\mathbf{X}\in\mathcal{X}^n$ is a vector of n sampled prompts and $\mathbf{Y}\in\mathcal{Y}^{n\times m}$ is a matrix of responses, with m responses for each of the n prompts; we explicitly write $\hat{\mathcal{J}}$ with the conventional expected reward maximization for notational convenience, though alternative objectives are not restricted.

Since the empirical problem (2) is a convex program with small size, it is now manageable. Combing with the projection step, we could write the program as a bi-level stochastic optimization:

$$\pi_\theta = \arg\min_{\pi_\theta\in\Pi_\theta} \mathbb{E}_x\left[\mathbb{KL}(\hat{\pi}^\star_{\mathbf{X},\mathbf{Y}_\theta}\|\pi_\theta)[x]\right] \quad \text{s.t. } \hat{\pi}^\star_{\mathbf{X},\mathbf{Y}_\theta} \in \arg\max_{\pi\in\Pi\cap\hat{\Phi}_+(\mathbf{X},\mathbf{Y}_\theta)} \hat{\mathcal{J}}(\pi;\mathbf{X},\mathbf{Y}_\theta) \tag{3}$$

where $\mathbf{Y}_\theta \sim \pi_\theta(\mathbf{X})$, hence $\hat{\pi}^\star$ is indirectly a function of θ.

Practical update. For general bi-level optimization problems, iteratively solving the upper and lower-level problems by alternatively fixing one while optimizing the other could be expensive (Zhang et al., 2024). We've however already setup a manageable inner problem, making it

Table 1: SFT methods from our optimization view. (w)-$\mathbb{XE}$ denotes (weighted) cross-entropy loss. RM stands for reward model. Binary reward indicates correctness. $\hat{\pi}^\star$ are (unnormalized) weights.

ALGO	loss $\mathcal{L}$	reward r	feasible set Φ	weight/acceptance $\hat{\pi}^\star$
(Iterative) SFT	$\mathbb{XE}$	constant	Π	constant
RFT	weighted $\mathbb{XE}$	binary	Π	$\mathbb{1}_{\{r(x,y)=1\}}$
RAFT (Best-of-N)	weighted $\mathbb{XE}$	RM	Π	$\mathbb{1}_{\{r(x_i,y)=\max_j r(x_i,y_{ij})\}}$
Ours	weighted $\mathbb{XE}$	Section 3	(2)	(2)

easy to solve for example using convex solvers. One could therefore do iterative gradient updates on the upper level while directly solving the lower-level at each iteration:

$$\theta' = \theta - \alpha \nabla_\theta \mathbb{E}_{x\sim\mu_{\mathbf{X}}}\left[\mathbb{KL}(\hat{\pi}^\star_{\mathbf{X},\mathbf{Y}_\theta} \| \pi_\theta)[x]\right] \quad \text{s.t. } \hat{\pi}^\star_{\mathbf{X},\mathbf{Y}_\theta} \in \arg\max_{\pi\in\Pi\cap\hat{\Phi}_+(\mathbf{X},\mathbf{Y}_\theta)} \hat{\mathcal{J}}(\pi;\mathbf{X},\mathbf{Y}_\theta) \quad (4)$$

where θ and θ' are the parameters of current and next iteration, respectively; and the projection step is also done with samples $(\mathbf{X}, \mathbf{Y}_\theta)$ of the current iteration.

Note that $\hat{\pi}^\star$ is indirectly a function of θ through the samples $(\mathbf{X}, \mathbf{Y}_\theta)$. The gradient $\nabla_\theta \mathbb{KL}(\hat{\pi}^\star_{\mathbf{X},\mathbf{Y}_\theta} \| \pi_\theta)$ hence requires differentiation through $\hat{\pi}^\star_{\mathbf{X},\mathbf{Y}_\theta}$, meaning differentiate through an $\arg\max$ operator, which can in principle be achieved through implicit differentiation (Amos & Kolter, 2017; Lorraine et al., 2020). However, to avoid additional implementation and computation overhead, instead we use the semi-gradient $\nabla_\theta \mathbb{KL}(\text{SG}\{\hat{\pi}^\star_{\mathbf{X},\mathbf{Y}_\theta}\} \| \pi_\theta)$, where $\text{SG}\{\cdot\}$ is a stop gradient operator. This stop-gradient trick is quite common in many ML applications (Sutton, 2018; Foerster et al., 2018; Chen & He, 2021), leading to the update:

$$\underbrace{\theta' = \theta - \alpha \nabla_\theta \mathbb{E}_{x\sim\mu_{\mathbf{X}}}\left[\mathbb{KL}(\text{SG}\{\hat{\pi}^\star_{\mathbf{X},\mathbf{Y}_\theta}\} \| \pi_\theta)[x]\right]}_{\text{approximate projection / weighted SFT}} \quad \text{s.t. } \underbrace{\hat{\pi}^\star_{\mathbf{X},\mathbf{Y}_\theta} \in \arg\max_{\pi\in\Pi\cap\hat{\Phi}_+(\mathbf{X},\mathbf{Y}_\theta)} \hat{\mathcal{J}}(\pi;\mathbf{X},\mathbf{Y}_\theta)}_{\text{optimization for weight}} \quad (5)$$

The semi-gradient $\nabla_\theta \mathbb{KL}(\text{SG}\{\hat{\pi}^\star\} \| \pi_\theta)[x_i] = -\sum_j \hat{\pi}^\star(y_{ij}|x_i) \frac{\partial}{\partial\theta} \log \pi_\theta(y_{ij}|x_i)$ is a weighted SFT update (via $\hat{\pi}^\star$). This observation creates a simple update with negligible implementation overhead.

Discussion. The update rule ended up aligning many iterative weighted SFT algorithms, such as RAFT (Dong et al., 2023) and RFT (Ouyang et al., 2022; Touvron et al., 2023). In hindsight, our algorithm is motivated by the observation that these extremely successful algorithms can be interpreted as projecting empirical solutions onto a parametric space. Consequently, it is reasonable to use the empirical estimate in (2), as RAFT and RFT have demonstrated strong practical performance despite the inherent bias introduced by the non-linearity of these estimations. Since it is essentially generalizes SFT by re-weighting a sample pair (x_i, y_{ij}) by $\hat{\pi}^\star(y_{ij}|x_i)$, at each iteration based on the solution of an optimization problem $\hat{\pi}^\star$, we create a Table 1 to outline the corresponding interpretation for some iterative SFT methods, from this optimization point-of-view.

The "inner" optimization for RFT/RAFT is trivial, as it assigns $\hat{\pi}^\star(y|x) = 1$ to accepted responses or to the response with the highest reward model score, respectively. Formulating these methods as optimization doesn't offer much benefits. However, this perspective provides flexibility for future work to extend our framework, allowing for feasible sets and weighting tailored to specific applications.

3 Practical Implementation

Yet, as we are working in an algorithm-agnostic fashion, we are now ready to select a specific RL algorithm, define its corresponding objective $\mathcal{J}$, and specify a reward function r.

Reward function. Since we are working on mathematical problem-solving, a ground-truth reward could be obtained through string matching (Cobbe et al., 2021; Hendrycks et al., 2021b) of the model's solution against the ground truth solution, yielding a binary reward function $r_{\text{match}} : \mathcal{X} \times \mathcal{Y} \to \{0, 1\}$ that indicates correctness. On top of the binary reward, we define our reward r_Δ as the reward margin. To formally construct the margin, we first define the expected reward of a set $\mathcal{G}$ such that $\bar{r}_\pi(x, \mathcal{G}) := \mathbb{E}_{y\sim\pi}[r_{\text{match}}(x, y) \mid y \in \mathcal{G}]$. We then define the reward margin r_Δ as the reward advantage of a group $\mathcal{G}$ against all other groups $\mathcal{Y} \setminus \mathcal{G}$:

$$r_\Delta(x, y \in \mathcal{G}) := \bar{r}_\pi(x, \mathcal{G}) - \bar{r}_\pi(x, \mathcal{Y} \setminus \mathcal{G}) \quad (6)$$

Table 2: An example of OPT_{IuB} compared to OPT_{cgpo}-(7)- with tie broken randomly, resulting in potentially non-unique $\hat{\pi}^\star$. This table shows several such $\hat{\pi}^\star$ solutions but not all. KL is omitted for brevity. Given the rewards below we have $\bar{r}(x_1, \mathcal{G}_\circ) = \bar{r}(x_1, \mathcal{G}_+) = \bar{r}(x_2, \mathcal{G}_+) = 1$ and $\bar{r}(x_2, \mathcal{G}_\circ) = 0.5$. Suppose the cap $q_+ = 0.5$, allowing at most 50% of accepted responses are extended $y \in \mathcal{G}_+$. For a solution matrix $\hat{\pi}^\star$, 1 and 0 represent accepted and rejected response, respectively.

prompt	**responses**	$r(x,y)$	$r_\Delta(x,y)$	$\hat{\pi}_1^\star = \text{OPT}_{\text{cgpo}}{}^\dagger$	$\hat{\pi}_2^\star = \text{OPT}_{\text{cgpo}}{}^\ddagger$	$\hat{\pi}^\star = \text{OPT}_{\text{IuB}}{}^\sharp$
x_1 (easy)	$y_{11}, y_{12} \in \mathcal{G}_\circ$ $y_{13}, y_{14} \in \mathcal{G}_+$	$\begin{pmatrix}1 & 1\\ 1 & 1\end{pmatrix}$	0 0	$\begin{pmatrix}0 & 0\\ 1 & 0\end{pmatrix}$	$\begin{pmatrix}0 & 0\\ 0 & 1\end{pmatrix}$	$\begin{pmatrix}1 & 0\\ 0 & 0\end{pmatrix}$
x_2 (hard)	$y_{21}, y_{22} \in \mathcal{G}_\circ$ $y_{23}, y_{24} \in \mathcal{G}_+$	$\begin{pmatrix}1 & 0\\ 1 & 1\end{pmatrix}$	-0.5 0.5	$\begin{pmatrix}1 & 0\\ 0 & 0\end{pmatrix}$	$\begin{pmatrix}0 & 0\\ 1 & 0\end{pmatrix}$	$\begin{pmatrix}0 & 0\\ 1 & 0\end{pmatrix}$

† CGPO case 1: for x_2 (hard), $y_{21} \in \mathcal{G}_\circ$ is accepted even though $\mathcal{G}_+$ has higher expected reward $\bar{r}(x_2, \mathcal{G}_+)$;
‡ CGPO case 2: y_{14} and y_{23} are both accepted, which exceeds the density budget $q_+ = 0.5$;
$^\sharp$ Ours: accepts y_{11} and y_{23} to maximize margin, $r_\Delta(x_2, y_{23}) = 0.5$, while adhering to the density cap $q_+ = 0.5$.

We have $r_\Delta(x, y \in \mathcal{G}_+) = \bar{r}_\pi(x, \mathcal{G}_+) - \bar{r}_\pi(x, \mathcal{G}_\circ)$, in our case, and similarly for $\mathcal{G}_\circ$. r_Δ may appear odd for not counting the correctness of individual y. This is handled subsequently.

RL objective. For the learning algorithm, our choice is Constraint Generative Policy Optimization (CGPO) (Xu et al., 2024b), which is designed for multi-objective constrained optimization of LLMs. The choice is driven by implementation considerations: CGPO's modular constraint-handling design makes it straightforward to incorporate additional constraints, such as the group density constraint in our case. CGPO in a nutshell can be viewed as a generalized Best-of-N (BoN), though depending on the specific CGPO settings. It operates by defining a feasible set Ξ over the sample space $\mathcal{X} \times \mathcal{Y}$, which are designed to capture constraint adherence for, e.g. correctness, factuality, and safety (Xu et al., 2024b). In short, $(x, y) \notin \Xi$ will be rejected. In the context of math reasoning, the objective of CGPO can be summarized as:

$$\max_\pi \mathbb{E}_x \mathbb{E}_{y\sim\pi}[r(x,y)] \quad \text{s.t. } \textstyle\sum_y [\pi(y|x) \mathbb{1}_{\{y \in \Xi_x\}}] \geq 1 \text{ for all } x$$
$$\text{where } \Xi_x := \underbrace{\{y : r_{\text{match}}(x,y) = 1\}}_{\text{correctness}} \cap \underbrace{\{y : \hat{\mathbb{KL}}(y; x, \pi_{\text{ref}}) \leq \mathbb{KL}_{\max}\}}_{\text{empirical KL}} \tag{7}$$

This objective essentially optimizes reward over the feasible sets Ξ_x such that feasible response y is correct and within an KL range of $\mathbb{KL}_{\max}$, where the KL constraint is measured using point estimate of the (forward) KL defined as $\hat{\mathbb{KL}}(y; x, \pi_{\text{ref}}) := \log \pi(y|x) - \log \pi_{\text{ref}}(y|x)$.

Resulted update. Recap our update is defined as $\theta' = \theta - \alpha \nabla_\theta \mathbb{E}_{x\sim\mu_{\mathbf{X}}} \left[\mathbb{KL}(\text{SG}\{\hat{\pi}^\star_{\mathbf{X},\mathbf{Y}_\theta}\} \| \pi_\theta)[x]\right]$ subject to $\hat{\pi}^\star_{\mathbf{X},\mathbf{Y}_\theta} \in \arg\max_{\pi \in \Pi \cap \hat{\Phi}_+(\mathbf{X},\mathbf{Y}_\theta)} \hat{\mathcal{J}}(\pi; \mathbf{X}, \mathbf{Y}_\theta)$. And we have now defined the RL objective $\mathcal{J}$ and the margin reward function r_Δ. We are now ready to put everything together:

$$\hat{\pi}^\star_{\mathbf{X},\mathbf{Y}_\theta} \in \arg\max_\pi \hat{\mathcal{J}}_\Delta(\pi; \mathbf{X}, \mathbf{Y}_\theta) := \tfrac{1}{nm} \textstyle\sum_i^n \sum_j^m [\pi(y_{ij}|x_i) r_\Delta(x_i, y_{ij})]$$
$$\underbrace{\text{s.t. } \pi \in \Pi \cap \hat{\Phi}_+(\mathbf{X}, \mathbf{Y}_\theta) \text{ and } \textstyle\sum_{y\in\mathbf{Y}_\theta} [\pi(y|x) \mathbb{1}_{\{y\in\Xi_x\}}] \geq 1 \text{ for all } x \in \mathbf{X}}_{\text{shorthanded as } \text{OPT}_{\text{IuB}} \text{ (inference under budget)}} \tag{8}$$

In addition, as CGPO is a generalization of BoN (with tie breaking randomly), $\hat{\pi}^\star$ will be a pure strategy, meaning at most one y will be accepted for each x, for subsequent projection (SFT).

Intuition. Behind this update our intuition can be verbally interpreted as: If a prompt x is hard, the margin of extended responses $r_\Delta(x, y \in \mathcal{G}_+) = \bar{r}_\pi(x, \mathcal{G}_+) - \bar{r}_\pi(x, \mathcal{G}_\circ)$ is likely to be large for $y \in \mathcal{G}_+$. Therefore $\hat{\pi}^\star$ will more likely to assign positive weight to an extended response $y \in \mathcal{G}_+$ so that the objective receive larger margin reward. In contrast, if a query x is simple, $r_\Delta(x, y \in \mathcal{G}_+)$ is likely to be small. Hence $\hat{\pi}^\star$ will possibly assign positive weight to regular responses $y \in \mathcal{G}_\circ$, so that one could save some density budget for harder queries. See a concrete example in Table 2.

Reward models. Note that the original CGPO has reward models for BoN ranking. We intentionally excludes reward models, in our OPT_{IuB} formulation as shown in (8), to highlight our methodological contributions, by decoupling reward modeling efforts. Nonetheless, using reward models remains possible. To avoid introducing additional notation, we elaborate verbally: OPT_{IuB} essentially selects either group $\mathcal{G}_+$ or $\mathcal{G}_\circ$ for a query x. Within a group $\mathcal{G}$, all responses receive the same $r_\Delta(x, \mathcal{G})$, leaving it possible to further rank responses within each group using reward models.

Algorithm 1 Inference Budget-Constrained Policy Optimization (IBPO)

Require: prompts $\mathbb{D}$, batch size n, num of responses m, init policy $\pi_0 = \pi_{\text{ref}}$, max iters T, cap q_+

for $t = 1, \ldots, T$ **do**
  prompt sampling & response generation: $\mathbf{X}^n \sim \mu_{\mathbb{D}}$, $\mathbf{Y}_\theta^{n\times m} \sim \pi_{\theta_t}(\mathbf{X})$
  evaluate correctness & empirical KL: $\mathbf{R}_{\text{c}}^{n\times m} = r_{\text{match}}(\mathbf{X}, \mathbf{Y})$, $\hat{\mathbf{KL}}^{n\times m} = \hat{\mathbb{KL}}(\mathbf{Y}; \mathbf{X}, \pi_{\text{ref}})$
  if CGPO (i.e. w/o IuB) **then**
    solve BoN ((7)): $\hat{\pi}^\star_{\mathbf{X},\mathbf{Y}_\theta} \in \text{OPT}_{\text{cgpo}}(\mathbf{X}, \mathbf{Y}_\theta, \mathbf{R}_{\text{c}}, \hat{\mathbf{KL}})$
  end if
  if IBPO (i.e. w/ IuB) **then**
    solve margin maximization ((8)): $\hat{\pi}^\star_{\mathbf{X},\mathbf{Y}_\theta} \in \text{OPT}_{\text{IUB}}(\mathbf{X}, \mathbf{Y}_\theta, \mathbf{R}_{\text{c}}, \hat{\mathbf{KL}}, q_+)$
  end if
  grad step: $-\sum_i \sum_j \hat{\pi}^\star_{\mathbf{X},\mathbf{Y}_\theta}(y_{ij}|x_i) \frac{\partial}{\partial\theta} \log \pi_\theta(y_{ij}|x_i)\big|_{\theta=\theta_t}$
end for

Implementation & solvers. A pseudo-code of our IBPO with OPT_{IuB} is listed in Algorithm 1. The key change is replacing the constrained reward ranking OPT_{CGPO} with a general optimization problem, in our case the margin maximization under budget denoted as OPT_{IuB}. The OPT_{IuB} problem is a (integer) linear program that could be solved by off-the-shelf solvers, such as CPLEX (Cplex, 2009), Gurobi (Gurobi Optimization, LLC, 2024), or SciPy (Virtanen et al., 2020) which is our choice.

4 Naïve Construction of $\mathcal{G}_+$

Yet we work on abstract $\mathcal{G}_\circ$ and $\mathcal{G}_+$. This section gives the details of our constructions of extended length responses, i.e. the group $\mathcal{G}_+$. Developing long reasoning models is beyond the scope of this work, as our focus is on the constrained optimization of LLMs. Our constructions are for demonstrative purpose only. Due to the intricate details and the space limit, we defer the full version of this section to Appendix B, including details of prompting, dataset construction, training pipelines, etc.

Figure 1 provides examples of our constructions. In a nutshell, we use the step CoT (SCoT) format from Dubey et al. (2024) as $\mathcal{G}_\circ$, and construct a sequential voting (SV) response as $\mathcal{G}_+$. SV serves as a unimodal baseline to demonstrate the performance of our construction. Adaptive SV (ASV) generates a mixture of SCoT and SV responses, allowing us to optimize its ability to adaptively choose between the two. For further details about the constructions, refer to Figure 1 and Appendix B.

Notations., we use LLaMA to refer to instruction-tuned LLaMA 3.1 8B (Dubey et al., 2024). ASV-SFT-α denotes ASV models that are supervise fine-tuned with a coefficient α (see Appendix B). ASV-IuB-q_+ refers to ASV models optimized by our Algorithm 1 with a budget constraint q_+.

5 Evaluation of IBPO w/ OPT_{IuB}

This section shows: (i) SV is a valid construction with reasonable improvement (Table 3) and scales as good as majority vote (MV, aka self-consistency (Wang et al., 2022)) (Figure 2a & 2b); (ii) ASV-SFT does not achieve good efficiency (Figure 2a & 2b) as SFT does not optimize it as an optimization objective; (iii) ASV-IuB optimized by IBPO achieves better efficiency (Figure 2a & 2b), adherence to constraints (Figure 2c), and allocation of inference to harder quires (Figure 2e & 2f).

5.1 Absolute Improvement (Table 3)

"Baselines". To put SV/ASV in comparison with other baselines in literature, we gather several baselines from the self-correction literature as essentially these methods increase inference length, though not extensively as Jaech et al. (2024). The results in Table 3 are mainly gathered from Qu et al. (2024); Kumar et al. (2024). The self-correction baselines often admit a multi-turn structure, similarly to the multi-trial construction of SV. We therefore include a column of inference cost measured by number of turns/trials for a rough comparison. The SFT comparators we include are (reproduced) Self-Refine (Madaan et al., 2024), STaR (Zelikman et al., 2022), S^3C (Yan et al.,

SV Prompt (Simplified)

You are asked to give at most eight diverse solutions in different way, without referencing to the previous trials.
If a solution occurs three times, it is considered as a consensus and will be used as the final answer.

ASV Prompt (Simplified)

For medium and hard level problems, you are asked to give at most eight diverse solutions in different way, without referencing to the previous trials.
For easy level problems, you are allowed only one attempt, which will be considered your final answer.

Voting Response $\mathcal{G}_+$ (SV, ASV Case 1)

[TRIAL] ## Step 1: ... steps omitted
The final answer is: $\boxed{\text{A1}}$. [/TRIAL]

[TRIAL] ## Step 1: ... steps omitted
The final answer is: $\boxed{\text{A2}}$. [/TRIAL]

[TRIAL] ## Step 1: ... steps omitted
The final answer is: $\boxed{\text{A1}}$. [/TRIAL]

[TRIAL] ## Step 1: ... steps omitted
The final answer is: $\boxed{\text{A1}}$. [/TRIAL]

The answer $\boxed{\text{A1}}$ has occurred three times, and is considered as a consensus.
The final answer is $\boxed{\text{A1}}$. I hope it is correct.

Non-Voting $\mathcal{G}_\circ$ (ASV Case 2)

[TRIAL] ## Step 1: ... steps omitted
The final answer is: $\boxed{\text{A1}}$. [/TRIAL]
Terminated due to difficulty level.

Table 3: Comparison of approaches on their improvements versus base models. †, ‡, †† indicate results duplicated from Qu et al. (2024); Yan et al. (2024); Kumar et al. (2024), respectively. * indicates our methods/constructions and the improvements are relative to LLaMA model.

approach	pass@1	improv.	turns/trials per response
SFT/Prompting-based			
SV-SFT*			
LLaMA	56.8	5.54	5.67x
ASV-SFT-1*			
LLaMA	55.6	4.43	5.74x
SFT-RISE†			
setting 1 (table 1 of †)	5.5	-0.3	5x
setting 2 (table 1 of †)	5.0	0.0	5x
SFT-SCoRe††			
setting 1 (table 1 of ††)	54.2	1.8	2x
setting 2 (table 1 of ††)	55.0	0.0	2x
RISE†			
LLaMA2 Base	1.4	-0.5	5x
+ boosting	5.5	0.0	5x
S^{3}C‡			
LLaMA3-8B	33.14	2.56	not studied
Mistral-7B	25.48	1.44	
DeepSeek-Math-Base-7B	41.40	3.18	
Qwen2-Math-7B	51.76	0.44	
Self-Refine†			
Base	1.9	0.0	3x
GPT-3.5	36.5	-3.2	3x
Mistral-7B	7.1	-0.4	3x
Eurus-7B-SFT	9.0	-3.3	3x
STaR††			
setting 1 (table 1 of ††)	54.0	0.4	2x
setting 2 (table 1 of ††)	41.2	-14.2	2x
Online Iterative/RL			
ASV-IuB-q_+*			
$q_+ = 25\%$	54.2	2.94	2.24x
$q_+ = 50\%$	55.4	4.14	2.16x
$q_+ = 75\%$	57.0	5.74	4.32x
RISE†			
+ Iteration 1	9.7	3.4	5x
+ Iteration 2	10.4	4.6	5x
SCoRe††			
Gemini 1.5 Flash	64.4	4.4	2x
+ more turns (fig. 8††)	≈66	≈6	5x-10x

Figure 1: Example of prompts and responses. For $\mathcal{G}_\circ$, we use standard step CoT (SCoT). To construct $\mathcal{G}_+$, the model is prompted to sequentially generate up to 8 trials encapsulated within the special tokens [TRIAL] and [/TRIAL], followed by a consensus answer. The SV prompt instructs the model to output only voting responses, allowing us to later evaluate its performance and show that it is a reasonable construction. The ASV prompt asks the model to decide whether to output a voting or non-voting response, facilitating our further optimization of budget allocation in Section 5.

2024), SFT-RI and SFT-SCoRe, where SFT-RI and SFT-SCoRe are SFT comparators implemented in Recursive Introspection (RI) (Qu et al., 2024) and SCoRe (Kumar et al., 2024) respectively.

ASV experiments. SV-SFT follows our training setup of Exp 1.2 in Table 7 (Appendix B). ASV-SFT-α follows our Exp 2.1 setup and is an adaptive baseline, meaning model decide whether to vote or not for a query. We report ASV-SFT-1 only as it is empirically the best ASV-SFT-α baseline, though still fall short in terms of efficiency. The ASV-IuB-q_+ experiments, initialized from ASV-SFT-1, are our RL-tuned adaptive models, optimized by IBPO with OPT_{IuB} as inner optimization.

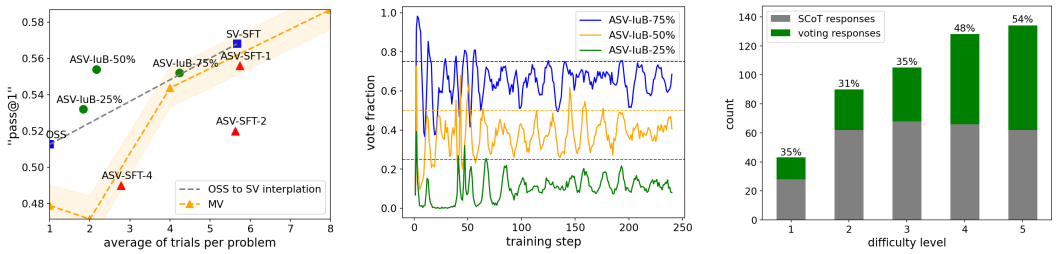

(a) performance of last checkpoints (c) vote ratio of correct responses (train set) (e) vote % by difficulty ($q_+ = 50\%$)

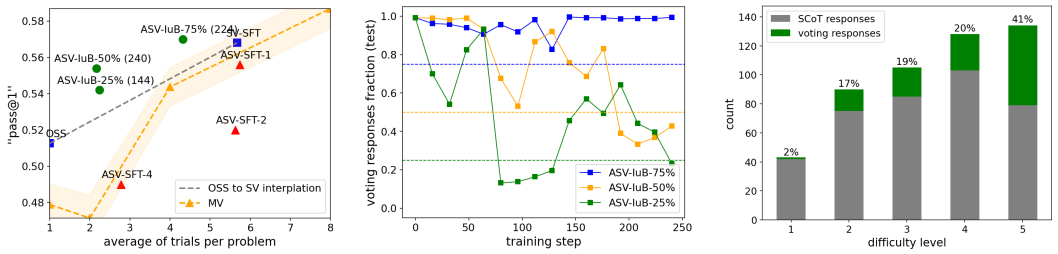

(b) best ones (steps in parentheses) (d) vote response ratio (test set) (f) vote % by difficulty ($q_+ = 25\%$)

Figure 2: Col 1: Comparison of pass@1 (maj@N for MV) against the average trials per response (x-axis). OSS refers to LLaMA. The interpolation between OSS and SV-SFT (aligning with MV) is a hypothetical efficiency boundary. ASV-SFT shows lower efficiency relative to this boundary, whereas ASV-IuB consistently achieves better efficiency (above the boundary). Col 2: Voting response ratio versus training steps. Dashed line denotes the budget q_+. On the training set, ASV-IuB follows the budget constraints exactly. Due to distribution shift, the constraint on testing set is not entirely exact, but still it is noticeable that the voting ratio follows the order of $75\% \succ 50\% \succ 25\%$. Col 3: ASV-IuB enables the model to dynamically allocate voting budget to harder problems.

Observations. We would like to emphasize that the comparison in Table 3 is not intended to demonstrate that SV outperforms SFT-based self-correction or that our ASV-IuB surpasses RL-based self-corrections. These efforts are orthogonal, as our focus is on constrained optimization. As observed, our SFT constructions—SV-SFT and ASV-SFT-1 achieve a clear improvement in pass@1 with high inference costs (5+ times the number of trials). The ASV-IuB-q_+ formulation, particularly with $q_+ = \{50\%, 75\%\}$, shows significant improvement while reducing costs by 4.14% at $2.16\times$ and 5.74% at $4.32\times$. This performance is on par with SCoRe, a state-of-the-art RL-based self-correction method. Note that the performance of ASV-IuB-q_+ is reported using the best checkpoints. Results from the last checkpoint are shown in Figure 2a. In addition, training curves are presented in Appendix F, which shows consistent improvements. As a somewhat tangential yet potentially intriguing observation, it is evident that prompting-based and SFT-based methods struggle with both absolute improvement (Table 3) and efficiency (Figure 2), supporting the conjecture that SFT alone does not enable self-correction (Huang et al., 2023; Kumar et al., 2024). This observation is also partially supported by concurrent work (DeepSeek-AI et al., 2025), which suggests that such self-correction emerges automatically during RL rather than manually created by prompting or SFT.

5.2 Efficiency, Budget Adherence & Allocation

Table 3 shows that our ASV-IuB-$q+$ models achieve results comparable to RL-based self-correction models, simply by inference budget management. In this subsection, we extend our discussion on: (i) performance-budget efficiency, (ii) constraint satisfaction, and (iii) inference budget allocation.

Performance-budget efficiency. In Figure 2a and 2b, we visually assess the performance-budget efficiency, compared to a hypothetical efficiency boundary. This boundary is an interpolation between OSS LLaMA model and SV-SFT. It is reasonable to consider it as a hypothetical boundary for two reasons: (i) OSS and SV-SFT are two extremes of ASV-IuB-q_+, corresponding to the cases of $q_+ = 0$ and $q_+ = 1$ respectively; and (ii) this interpolation achieves an increase comparable to MV, if not slightly better. The SFT version of ASV is generally much worse than the boundary,

as SFT alone does not optimize resource allocation as a mathematical objective. For ASV-IuB-q_+ optimized by IBPO, we report both the last and best checkpoint results in Figure 2a and Figure 2b, respectively. Our formulation achieves, in general, better performance-budget efficiency, except $q_+ = 75\%$ in Figure 2a. We will extend our discussion on this unsuccessful case soon.

Constraint satisfaction. We then evaluate how effectively the constraints are enforced. In Figure 2c, the budget constraints are successfully maintained during training for $q_+ = \{25\%, 50\%, 75\%\}$. Due to distribution shifts, exact adherence to these constraints is not expected on the test set. Nevertheless, Figure 2d demonstrates that constraints are still upheld at the end of training for $q_+ = \{25\%, 50\%\}$, and the ratio of voting responses follows the order $75\% \succ 50\% \succ 25\%$. (Figure 2c illustrates that our model meets the budget constraints for the set of correct responses. The constraints also hold for all responses, see Appendix F.)

Difficulty-adaptive allocation. We have show improved efficiency and adherence to constraints, we would like to further validate the intuition of our design: that more challenging problems may require longer reasoning steps, whereas simpler problems can be resolved with just SCoT responses. Ideally, the model should allocate more voting responses to problems with higher difficulty levels. To this end, we use the difficulty levels from the metadata of Hendrycks MATH and plot the ratio of voting responses for each difficulty level. Figure 2f and 2e illustrates that for both $q_+ = \{25\%, 50\%\}$, more challenging problems, such as those at levels 4 and 5, receive a higher allocation of budgets. This allocation pattern is particularly evident for the case of $q_+ = 25\%$, where only 2% of level 1 problems receive voting responses.

Discussion on the unsuccessful case. There is one unsuccessful case in Figure 2a: the last checkpoint of ASV-IuB-75%, which falls on the hypothetical boundary rather than above it. This outcome is arguably expected, as observed in Figure 2d, where ASV-IuB-75% outputs almost exclusively voting responses at the end of training. As a result, this model is not adaptively allocating resources, and thus no improvement in efficiency is anticipated. This unsuccessful case is hence caused by the distribution shift between the training set and the testing set. It is possible that scaling the training set—given that our training set $\mathbb{D}_{\text{RL}}$ contains approximately 10k prompts, which is relatively small—will make the testing set more likely to be in-distribution and thereby alleviate such issue.

6 Conclusion & Discussions

We derived a constrained policy optimization framework, IBPO, from an optimization perspective, resulting in a simple weighted SFT update that resembles successful iterative SFT algorithms such as RFT and RAFT. In each iteration, the optimal weight is obtained by solving an (integer) linear program. The practical implementation of IBPO is build on top of CGPO, and is evaluated on a math reasoning task with inference budget constraints. Empirical evaluations show that our framework enables the model to adhere to constraints and dynamically allocate the inference budget.

Batch optimization & solver time. Since we solve an optimization problem per iteration (i.e. per mini-batch), limited computational resources can result in smaller sample sizes for the inner optimization problem, leading to larger variance. This issue can be mitigated through "sample accumulation", accumulating samples across multiple consecutive steps, similar to gradient accumulation practice in LLMs. A pseudo-code for sample accumulation can be found in Appendix D. In addition, though integer linear programming is NP-hard (Vazirani, 1997), the number of variables in our batch-level optimization is typically small, resulting in minimal computational overhead. Refer to the wall-time plot for the SciPy solver in Appendix D for details.

Broader applications. Our framework has only been evaluated with inference in math, the resource allocation problem however has far-reaching implications within the ML community. As a result, our framework can be potentially extended to further applications. For instance, a potential application is statistical parity (Zemel et al., 2013), aka group fairness. In this context, one could consider attributing responses to their respective social groups, and cap the density of responses that correspond to socially privileged groups, to encourage more inclusive and equitable responses across different demographics. Another potential application is the balanced expert activation in mixture of experts (Jacobs et al., 1991; Shazeer et al., 2017; Lepikhin et al., 2020) systems, which is sometimes achieved by adding an auxiliary balancing loss (Wei et al., 2024). Alternatively, this balance can be possibly achieved by enforcing a minimal activation density for each expert. This may help to pre-

vent over-reliance on a subset of experts, and thus enhancing the overall robustness and efficiency. We leave the exploration of broader applications and their implementations as future directions.

REFERENCES

Pranjal Aggarwal, Aman Madaan, Yiming Yang, et al. Let's sample step by step: Adaptive-consistency for efficient reasoning and coding with llms. *arXiv preprint arXiv:2305.11860*, 2023.

Eitan Altman. *Constrained Markov decision processes*. Routledge, 2021.

Brandon Amos and J Zico Kolter. Optnet: Differentiable optimization as a layer in neural networks. In *International conference on machine learning*, pp. 136–145. PMLR, 2017.

Lasse F Wolff Anthony, Benjamin Kanding, and Raghavendra Selvan. Carbontracker: Tracking and predicting the carbon footprint of training deep learning models. *arXiv preprint arXiv:2007.03051*, 2020.

Jacob Austin, Augustus Odena, Maxwell Nye, Maarten Bosma, Henryk Michalewski, David Dohan, Ellen Jiang, Carrie Cai, Michael Terry, Quoc Le, et al. Program synthesis with large language models. *arXiv preprint arXiv:2108.07732*, 2021.

Ashwinkumar Badanidiyuru, Robert Kleinberg, and Aleksandrs Slivkins. Bandits with knapsacks. *Journal of the ACM (JACM)*, 65(3):1–55, 2018.

Sébastien Bubeck, Ofer Dekel, Tomer Koren, and Yuval Peres. Bandit convex optimization:\sqrtt regret in one dimension. In *Conference on Learning Theory*, pp. 266–278. PMLR, 2015.

Semih Cayci, Yilin Zheng, and Atilla Eryilmaz. A lyapunov-based methodology for constrained optimization with bandit feedback. In *Proceedings of the AAAI Conference on Artificial Intelligence*, volume 36, pp. 3716–3723, 2022.

Mark Chen, Jerry Tworek, Heewoo Jun, Qiming Yuan, Henrique Ponde De Oliveira Pinto, Jared Kaplan, Harri Edwards, Yuri Burda, Nicholas Joseph, Greg Brockman, et al. Evaluating large language models trained on code. *arXiv preprint arXiv:2107.03374*, 2021.

Xinlei Chen and Kaiming He. Exploring simple siamese representation learning. In *Proceedings of the IEEE/CVF conference on computer vision and pattern recognition*, pp. 15750–15758, 2021.

Hollis B Chenery and Kenneth S Kretschmer. Resource allocation for economic development. *Econometrica, Journal of the Econometric Society*, pp. 365–399, 1956.

Nuttapong Chentanez, Andrew Barto, and Satinder Singh. Intrinsically motivated reinforcement learning. *Advances in neural information processing systems*, 17, 2004.

Yinlam Chow, Ofir Nachum, Edgar Duenez-Guzman, and Mohammad Ghavamzadeh. A lyapunov-based approach to safe reinforcement learning. *Advances in neural information processing systems*, 31, 2018.

Karl Cobbe, Vineet Kosaraju, Mohammad Bavarian, Mark Chen, Heewoo Jun, Lukasz Kaiser, Matthias Plappert, Jerry Tworek, Jacob Hilton, Reiichiro Nakano, et al. Training verifiers to solve math word problems. *arXiv preprint arXiv:2110.14168*, 2021.

IBM ILOG Cplex. V12. 1: User's manual for cplex. *International Business Machines Corporation*, 46(53):157, 2009.

DeepSeek-AI, Daya Guo, Dejian Yang, Haowei Zhang, Junxiao Song, Ruoyu Zhang, Runxin Xu, Qihao Zhu, Shirong Ma, Peiyi Wang, Xiao Bi, Xiaokang Zhang, Xingkai Yu, Yu Wu, Z. F. Wu, Zhibin Gou, Zhihong Shao, Zhuoshu Li, Ziyi Gao, Aixin Liu, Bing Xue, Bingxuan Wang, Bochao Wu, Bei Feng, Chengda Lu, Chenggang Zhao, Chengqi Deng, Chenyu Zhang, Chong Ruan, Damai Dai, Deli Chen, Dongjie Ji, Erhang Li, Fangyun Lin, Fucong Dai, Fuli Luo, Guangbo Hao, Guanting Chen, Guowei Li, H. Zhang, Han Bao, Hanwei Xu, Haocheng Wang, Honghui Ding, Huajian Xin, Huazuo Gao, Hui Qu, Hui Li, Jianzhong Guo, Jiashi Li, Jiawei Wang, Jingchang Chen, Jingyang Yuan, Junjie Qiu, Junlong Li, J. L. Cai, Jiaqi Ni, Jian Liang, Jin Chen, Kai

Dong, Kai Hu, Kaige Gao, Kang Guan, Kexin Huang, Kuai Yu, Lean Wang, Lecong Zhang, Liang Zhao, Litong Wang, Liyue Zhang, Lei Xu, Leyi Xia, Mingchuan Zhang, Minghua Zhang, Minghui Tang, Meng Li, Miaojun Wang, Mingming Li, Ning Tian, Panpan Huang, Peng Zhang, Qiancheng Wang, Qinyu Chen, Qiushi Du, Ruiqi Ge, Ruisong Zhang, Ruizhe Pan, Runji Wang, R. J. Chen, R. L. Jin, Ruyi Chen, Shanghao Lu, Shangyan Zhou, Shanhuang Chen, Shengfeng Ye, Shiyu Wang, Shuiping Yu, Shunfeng Zhou, Shuting Pan, S. S. Li, Shuang Zhou, Shaoqing Wu, Shengfeng Ye, Tao Yun, Tian Pei, Tianyu Sun, T. Wang, Wangding Zeng, Wanjia Zhao, Wen Liu, Wenfeng Liang, Wenjun Gao, Wenqin Yu, Wentao Zhang, W. L. Xiao, Wei An, Xiaodong Liu, Xiaohan Wang, Xiaokang Chen, Xiaotao Nie, Xin Cheng, Xin Liu, Xin Xie, Xingchao Liu, Xinyu Yang, Xinyuan Li, Xuecheng Su, Xuheng Lin, X. Q. Li, Xiangyue Jin, Xiaojin Shen, Xiaosha Chen, Xiaowen Sun, Xiaoxiang Wang, Xinnan Song, Xinyi Zhou, Xianzu Wang, Xinxia Shan, Y. K. Li, Y. Q. Wang, Y. X. Wei, Yang Zhang, Yanhong Xu, Yao Li, Yao Zhao, Yaofeng Sun, Yaohui Wang, Yi Yu, Yichao Zhang, Yifan Shi, Yiliang Xiong, Ying He, Yishi Piao, Yisong Wang, Yixuan Tan, Yiyang Ma, Yiyuan Liu, Yongqiang Guo, Yuan Ou, Yuduan Wang, Yue Gong, Yuheng Zou, Yujia He, Yunfan Xiong, Yuxiang Luo, Yuxiang You, Yuxuan Liu, Yuyang Zhou, Y. X. Zhu, Yanhong Xu, Yanping Huang, Yaohui Li, Yi Zheng, Yuchen Zhu, Yunxian Ma, Ying Tang, Yukun Zha, Yuting Yan, Z. Z. Ren, Zehui Ren, Zhangli Sha, Zhe Fu, Zhean Xu, Zhenda Xie, Zhengyan Zhang, Zhewen Hao, Zhicheng Ma, Zhigang Yan, Zhiyu Wu, Zihui Gu, Zijia Zhu, Zijun Liu, Zilin Li, Ziwei Xie, Ziyang Song, Zizheng Pan, Zhen Huang, Zhipeng Xu, Zhongyu Zhang, and Zhen Zhang. Deepseek-r1: Incentivizing reasoning capability in llms via reinforcement learning, 2025. URL https://arxiv.org/abs/2501.12948.

Eric V Denardo. On linear programming in a markov decision problem. *Management Science*, 16 (5):281–288, 1970.

Hanze Dong, Wei Xiong, Deepanshu Goyal, Yihan Zhang, Winnie Chow, Rui Pan, Shizhe Diao, Jipeng Zhang, Kashun Shum, and Tong Zhang. Raft: Reward ranked finetuning for generative foundation model alignment. *arXiv preprint arXiv:2304.06767*, 2023.

Abhimanyu Dubey, Abhinav Jauhri, Abhinav Pandey, Abhishek Kadian, Ahmad Al-Dahle, Aiesha Letman, Akhil Mathur, Alan Schelten, Amy Yang, Angela Fan, et al. The llama 3 herd of models. *arXiv preprint arXiv:2407.21783*, 2024.

Abraham D Flaxman, Adam Tauman Kalai, and H Brendan McMahan. Online convex optimization in the bandit setting: gradient descent without a gradient. *arXiv preprint cs/0408007*, 2004.

Jakob Foerster, Gregory Farquhar, Maruan Al-Shedivat, Tim Rocktäschel, Eric Xing, and Shimon Whiteson. Dice: The infinitely differentiable monte carlo estimator. In *International Conference on Machine Learning*, pp. 1529–1538. PMLR, 2018.

Javier Garcıa and Fernando Fernández. A comprehensive survey on safe reinforcement learning. *Journal of Machine Learning Research*, 16(1):1437–1480, 2015.

Gurobi Optimization, LLC. Gurobi Optimizer Reference Manual, 2024. URL https://www.gurobi.com.

Tuomas Haarnoja, Haoran Tang, Pieter Abbeel, and Sergey Levine. Reinforcement learning with deep energy-based policies. In *International conference on machine learning*, pp. 1352–1361. PMLR, 2017.

Tuomas Haarnoja, Aurick Zhou, Pieter Abbeel, and Sergey Levine. Soft actor-critic: Off-policy maximum entropy deep reinforcement learning with a stochastic actor. In *International conference on machine learning*, pp. 1861–1870. PMLR, 2018.

Elad Hazan et al. Introduction to online convex optimization. *Foundations and Trends® in Optimization*, 2(3-4):157–325, 2016.

Peter Henderson, Jieru Hu, Joshua Romoff, Emma Brunskill, Dan Jurafsky, and Joelle Pineau. Towards the systematic reporting of the energy and carbon footprints of machine learning. *Journal of Machine Learning Research*, 21(248):1–43, 2020.

Dan Hendrycks, Steven Basart, Saurav Kadavath, Mantas Mazeika, Akul Arora, Ethan Guo, Collin Burns, Samir Puranik, Horace He, Dawn Song, et al. Measuring coding challenge competence with apps. *arXiv preprint arXiv:2105.09938*, 2021a.

Dan Hendrycks, Collin Burns, Saurav Kadavath, Akul Arora, Steven Basart, Eric Tang, Dawn Song, and Jacob Steinhardt. Measuring mathematical problem solving with the math dataset. *arXiv preprint arXiv:2103.03874*, 2021b.

Jie Huang, Xinyun Chen, Swaroop Mishra, Huaixiu Steven Zheng, Adams Wei Yu, Xinying Song, and Denny Zhou. Large language models cannot self-correct reasoning yet. *arXiv preprint arXiv:2310.01798*, 2023.

Toshihide Ibaraki and Naoki Katoh. *Resource allocation problems: algorithmic approaches*. MIT press, 1988.

Robert A Jacobs, Michael I Jordan, Steven J Nowlan, and Geoffrey E Hinton. Adaptive mixtures of local experts. *Neural computation*, 3(1):79–87, 1991.

Aaron Jaech, Adam Kalai, Adam Lerer, Adam Richardson, Ahmed El-Kishky, Aiden Low, Alec Helyar, Aleksander Madry, Alex Beutel, Alex Carney, et al. Openai o1 system card. *arXiv preprint arXiv:2412.16720*, 2024.

Mingyu Jin, Qinkai Yu, Dong Shu, Haiyan Zhao, Wenyue Hua, Yanda Meng, Yongfeng Zhang, and Mengnan Du. The impact of reasoning step length on large language models. *arXiv preprint arXiv:2401.04925*, 2024.

Samuel Karlin. *Mathematical methods and theory in games, programming, and economics*, volume 2. Courier Corporation, 2003.

Jacek Karwowski, Oliver Hayman, Xingjian Bai, Klaus Kiendlhofer, Charlie Griffin, and Joar Skalse. Goodhart's law in reinforcement learning. *arXiv preprint arXiv:2310.09144*, 2023.

Aviral Kumar, Vincent Zhuang, Rishabh Agarwal, Yi Su, John D Co-Reyes, Avi Singh, Kate Baumli, Shariq Iqbal, Colton Bishop, Rebecca Roelofs, et al. Training language models to self-correct via reinforcement learning. *arXiv preprint arXiv:2409.12917*, 2024.

Xin Lai, Zhuotao Tian, Yukang Chen, Senqiao Yang, Xiangru Peng, and Jiaya Jia. Step-dpo: Step-wise preference optimization for long-chain reasoning of llms. *arXiv preprint arXiv:2406.18629*, 2024.

Dmitry Lepikhin, HyoukJoong Lee, Yuanzhong Xu, Dehao Chen, Orhan Firat, Yanping Huang, Maxim Krikun, Noam Shazeer, and Zhifeng Chen. Gshard: Scaling giant models with conditional computation and automatic sharding. *arXiv preprint arXiv:2006.16668*, 2020.

Tian Liang, Zhiwei He, Wenxiang Jiao, Xing Wang, Yan Wang, Rui Wang, Yujiu Yang, Shuming Shi, and Zhaopeng Tu. Encouraging divergent thinking in large language models through multi-agent debate. *arXiv preprint arXiv:2305.19118*, 2023.

Hunter Lightman, Vineet Kosaraju, Yura Burda, Harri Edwards, Bowen Baker, Teddy Lee, Jan Leike, John Schulman, Ilya Sutskever, and Karl Cobbe. Let's verify step by step. *arXiv preprint arXiv:2305.20050*, 2023.

Evan Z Liu, Aditi Raghunathan, Percy Liang, and Chelsea Finn. Decoupling exploration and exploitation for meta-reinforcement learning without sacrifices. In *International conference on machine learning*, pp. 6925–6935. PMLR, 2021.

Jonathan Lorraine, Paul Vicol, and David Duvenaud. Optimizing millions of hyperparameters by implicit differentiation. In *International conference on artificial intelligence and statistics*, pp. 1540–1552. PMLR, 2020.

Aman Madaan, Niket Tandon, Prakhar Gupta, Skyler Hallinan, Luyu Gao, Sarah Wiegreffe, Uri Alon, Nouha Dziri, Shrimai Prabhumoye, Yiming Yang, et al. Self-refine: Iterative refinement with self-feedback. *Advances in Neural Information Processing Systems*, 36, 2024.

Alan S Manne. Linear programming and sequential decisions. *Management Science*, 6(3):259–267, 1960.

William H Montgomery and Sergey Levine. Guided policy search via approximate mirror descent. *Advances in Neural Information Processing Systems*, 29, 2016.

Ofir Nachum and Bo Dai. Reinforcement learning via fenchel-rockafellar duality. *arXiv preprint arXiv:2001.01866*, 2020.

Ofir Nachum, Yinlam Chow, Bo Dai, and Lihong Li. Dualdice: Behavior-agnostic estimation of discounted stationary distribution corrections. *Advances in neural information processing systems*, 32, 2019.

Long Ouyang, Jeffrey Wu, Xu Jiang, Diogo Almeida, Carroll Wainwright, Pamela Mishkin, Chong Zhang, Sandhini Agarwal, Katarina Slama, Alex Ray, et al. Training language models to follow instructions with human feedback. *Advances in neural information processing systems*, 35: 27730–27744, 2022.

Alexander Pan, Kush Bhatia, and Jacob Steinhardt. The effects of reward misspecification: Mapping and mitigating misaligned models. *arXiv preprint arXiv:2201.03544*, 2022.

Deepak Pathak, Pulkit Agrawal, Alexei A Efros, and Trevor Darrell. Curiosity-driven exploration by self-supervised prediction. In *International conference on machine learning*, pp. 2778–2787. PMLR, 2017.

Xue Bin Peng, Aviral Kumar, Grace Zhang, and Sergey Levine. Advantage-weighted regression: Simple and scalable off-policy reinforcement learning. *arXiv preprint arXiv:1910.00177*, 2019.

Jan Peters, Katharina Mulling, and Yasemin Altun. Relative entropy policy search. In *Proceedings of the AAAI Conference on Artificial Intelligence*, volume 24, pp. 1607–1612, 2010.

Chau Pham, Boyi Liu, Yingxiang Yang, Zhengyu Chen, Tianyi Liu, Jianbo Yuan, Bryan A Plummer, Zhaoran Wang, and Hongxia Yang. Let models speak ciphers: Multiagent debate through embeddings. *arXiv preprint arXiv:2310.06272*, 2023.

Yuxiao Qu, Tianjun Zhang, Naman Garg, and Aviral Kumar. Recursive introspection: Teaching language model agents how to self-improve. *arXiv preprint arXiv:2407.18219*, 2024.

Rafael Rafailov, Archit Sharma, Eric Mitchell, Christopher D Manning, Stefano Ermon, and Chelsea Finn. Direct preference optimization: Your language model is secretly a reward model. *Advances in Neural Information Processing Systems*, 36, 2024.

Alex Ray, Joshua Achiam, and Dario Amodei. Benchmarking safe exploration in deep reinforcement learning. *arXiv preprint arXiv:1910.01708*, 7(1):2, 2019.

Noam Shazeer, Azalia Mirhoseini, Krzysztof Maziarz, Andy Davis, Quoc Le, Geoffrey Hinton, and Jeff Dean. Outrageously large neural networks: The sparsely-gated mixture-of-experts layer. *arXiv preprint arXiv:1701.06538*, 2017.

Joar Skalse, Nikolaus Howe, Dmitrii Krasheninnikov, and David Krueger. Defining and characterizing reward gaming. *Advances in Neural Information Processing Systems*, 35:9460–9471, 2022.

Aleksandrs Slivkins et al. Introduction to multi-armed bandits. *Foundations and Trends® in Machine Learning*, 12(1-2):1–286, 2019.

Charlie Snell, Ilya Kostrikov, Yi Su, Mengjiao Yang, and Sergey Levine. Offline rl for natural language generation with implicit language q learning. *arXiv preprint arXiv:2206.11871*, 2022.

Charlie Snell, Jaehoon Lee, Kelvin Xu, and Aviral Kumar. Scaling llm test-time compute optimally can be more effective than scaling model parameters. *arXiv preprint arXiv:2408.03314*, 2024.

Richard S Sutton. Reinforcement learning: An introduction. *A Bradford Book*, 2018.

Hugo Touvron, Louis Martin, Kevin Stone, Peter Albert, Amjad Almahairi, Yasmine Babaei, Nikolay Bashlykov, Soumya Batra, Prajjwal Bhargava, Shruti Bhosale, et al. Llama 2: Open foundation and fine-tuned chat models. *arXiv preprint arXiv:2307.09288*, 2023.

Vijay V Vazirani. Approximation algorithms. *Georgia Inst. Tech*, 1997.

Pauli Virtanen, Ralf Gommers, Travis E. Oliphant, Matt Haberland, Tyler Reddy, David Cournapeau, Evgeni Burovski, Pearu Peterson, Warren Weckesser, Jonathan Bright, Stéfan J. van der Walt, Matthew Brett, Joshua Wilson, K. Jarrod Millman, Nikolay Mayorov, Andrew R. J. Nelson, Eric Jones, Robert Kern, Eric Larson, C J Carey, İlhan Polat, Yu Feng, Eric W. Moore, Jake VanderPlas, Denis Laxalde, Josef Perktold, Robert Cimrman, Ian Henriksen, E. A. Quintero, Charles R. Harris, Anne M. Archibald, Antônio H. Ribeiro, Fabian Pedregosa, Paul van Mulbregt, and SciPy 1.0 Contributors. SciPy 1.0: Fundamental Algorithms for Scientific Computing in Python. *Nature Methods*, 17:261–272, 2020. doi: 10.1038/s41592-019-0686-2.

Xinglin Wang, Shaoxiong Feng, Yiwei Li, Peiwen Yuan, Yueqi Zhang, Boyuan Pan, Heda Wang, Yao Hu, and Kan Li. Make every penny count: Difficulty-adaptive self-consistency for cost-efficient reasoning. *arXiv preprint arXiv:2408.13457*, 2024.

Xuezhi Wang, Jason Wei, Dale Schuurmans, Quoc Le, Ed Chi, Sharan Narang, Aakanksha Chowdhery, and Denny Zhou. Self-consistency improves chain of thought reasoning in language models. *arXiv preprint arXiv:2203.11171*, 2022.

Jason Wei, Xuezhi Wang, Dale Schuurmans, Maarten Bosma, Fei Xia, Ed Chi, Quoc V Le, Denny Zhou, et al. Chain-of-thought prompting elicits reasoning in large language models. *Advances in neural information processing systems*, 35:24824–24837, 2022.

Tianwen Wei, Bo Zhu, Liang Zhao, Cheng Cheng, Biye Li, Weiwei Lü, Peng Cheng, Jianhao Zhang, Xiaoyu Zhang, Liang Zeng, et al. Skywork-moe: A deep dive into training techniques for mixture-of-experts language models. *arXiv preprint arXiv:2406.06563*, 2024.

Mayi Xu, Yongqi Li, Ke Sun, and Tieyun Qian. Adaption-of-thought: Learning question difficulty improves large language models for reasoning. In *Proceedings of the 2024 Conference on Empirical Methods in Natural Language Processing*, pp. 5468–5495, 2024a.

Tengyu Xu, Eryk Helenowski, Karthik Abinav Sankararaman, Di Jin, Kaiyan Peng, Eric Han, Shaoliang Nie, Chen Zhu, Hejia Zhang, Wenxuan Zhou, et al. The perfect blend: Redefining rlhf with mixture of judges. *arXiv preprint arXiv:2409.20370*, 2024b.

Yuchen Yan, Jin Jiang, Yang Liu, Yixin Cao, Xin Xu, Xunliang Cai, Jian Shao, et al. S^3c-math: Spontaneous step-level self-correction makes large language models better mathematical reasoners. *arXiv preprint arXiv:2409.01524*, 2024.

Tsung-Yen Yang, Justinian Rosca, Karthik Narasimhan, and Peter J Ramadge. Projection-based constrained policy optimization. *arXiv preprint arXiv:2010.03152*, 2020.

Zishun Yu, Yunzhe Tao, Liyu Chen, Tao Sun, and Hongxia Yang. $\mathcal{B}$-coder: On value-based deep reinforcement learning for program synthesis. In *The Twelfth International Conference on Learning Representations*, 2023.

Eric Zelikman, Yuhuai Wu, Jesse Mu, and Noah Goodman. Star: Bootstrapping reasoning with reasoning. *Advances in Neural Information Processing Systems*, 35:15476–15488, 2022.

Rich Zemel, Yu Wu, Kevin Swersky, Toni Pitassi, and Cynthia Dwork. Learning fair representations. In *International conference on machine learning*, pp. 325–333. PMLR, 2013.

Yihua Zhang, Prashant Khanduri, Ioannis Tsaknakis, Yuguang Yao, Mingyi Hong, and Sijia Liu. An introduction to bilevel optimization: Foundations and applications in signal processing and machine learning. *IEEE Signal Processing Magazine*, 41(1):38–59, 2024.

Yiming Zhang, Quan Vuong, and Keith Ross. First order constrained optimization in policy space. *Advances in Neural Information Processing Systems*, 33:15338–15349, 2020.

Brian D Ziebart. *Modeling purposeful adaptive behavior with the principle of maximum causal entropy*. Carnegie Mellon University, 2010.

Daniel M Ziegler, Nisan Stiennon, Jeffrey Wu, Tom B Brown, Alec Radford, Dario Amodei, Paul Christiano, and Geoffrey Irving. Fine-tuning language models from human preferences. *arXiv preprint arXiv:1909.08593*, 2019.

Martin Zinkevich. Online convex programming and generalized infinitesimal gradient ascent. In *Proceedings of the 20th international conference on machine learning (icml-03)*, pp. 928–936, 2003.

A Motivating Example

Figure 3 is an example that advanced reasoning model spent more than enough time on a trivial problem.

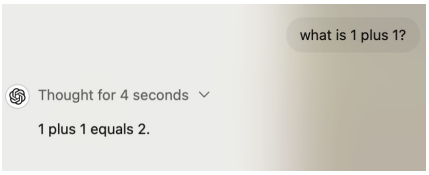

Figure 3: A long reasoning-chain model spent more than enough inference time on a trivial problem.

B Full Version of Section 4: Acronyms, Naïve Construction of $\mathcal{G}_+$ & Training Pipelines

Yet we work on abstract groups $\mathcal{G}_\circ$ and $\mathcal{G}_+$. In this section, we present the details of our constructions of extended length responses, i.e. the extended group $\mathcal{G}_+$. However developing long reasoning models is beyond the scope of this work, as our focus is on the constrained optimization of LLMs. Our constructions are for demonstrative purpose only. Due to the intricate details involved in prompts, datasets, and training pipelines, this section may appear somewhat dense. To make it more approachable, we have structured our writing in a way that readers can, if they wish, focus on the broader ideas without delving deeply into the specifics of constructions. A TL;DR version of this section is provided below.

TL;DR. We construct two types of illustrative extended responses: Sequential Voting (SV) and Adaptive Sequential Voting (ASV). Figure 4 visually explains how these constructions are implemented. The goal of the SV is to establish a baseline that generates only responses in $\mathcal{G}_+$, thereby serving as an uni-modal comparator. SV scales roughly as well as vanilla majority voting (MV), aka self-consistency (Wang et al., 2022). In contrast, ASV outputs a mixture of responses of $y \in \mathcal{G}_\circ$ and $y \in \mathcal{G}_+$. This allows the model to adaptively decide which type of response to produce based on the query. The goal of ASV is to further enable IBPO optimization, as IBPO implicitly assumes the model generates both regular and extended-length responses. In Section 5, we show that ASV optimized by IBPO, achieves better allocation of the inference budget.

B.1 Construction of Sequential Vote

Acronyms. For clarity, we explicitly define key terms to hopefully resolve any potential ambiguities. *Response*: A response refers to a sequence generated until a terminal token is encountered. For precision, we sometimes refer to these as voting responses or SCoT responses, as illustrated in Figure 4, after introducing our sequential voting baselines. *Trial*: A trial denotes a solution instance, which is demarcated by the special tokens [TRIAL] ... [/TRIAL], as shown in the voting response example in Figure 4. While a voting response contains multiple trials, a SCoT response or a non-voting response contains exactly one trial, as also depicted in Figure 4.

SCoT Prompt + Cond.

Solve the following math problem efficiently and clearly:
- For simple problems (2 steps or fewer):
Provide a concise solution with minimal explanation.
- For complex problems (3 steps or more):
Use this step-by-step format:
Step 1: [Concise description]
[Brief explanation and calculations]
Step 2: [Concise description]
[Brief explanation and calculations]
...
Regardless of the approach, always conclude with:
Therefore, the final answer is: $\\boxed{answer}$. I hope it is correct.
Where [answer] is just the final number or expression that solves the problem.
[Condition Description]
Problem: {{ problem }}

SCoT Response

Step 1: ... steps omitted
The final answer is: $\boxed{\text{A1}}$. I hope it is correct.

SV Cond.

You are asked to give at most eight diverse solutions in different way, without referencing to the previous trials.
Each trial should be contained in a separate [TRIAL] trial solution [/TRIAL] block.
If a solution occurs three times, it is considered as a consensus and will be used as the final answer.
If there is no consensus, use the solution from the most plausible trial.

ASV Cond.

For medium and hard level problems, you are asked to give at most eight diverse solutions in different way, without referencing to the previous trials.
Each trial should be contained in a separate [TRIAL] trial solution [/TRIAL] block.
If a solution occurs three times, it is considered as a consensus and will be used as the final answer.
If there is no consensus, use the solution from the most plausible trial.
For easy level problems, you are allowed only one attempt, which will be considered your final answer.

Voting Response (SV, ASV Case 1)

[TRIAL] ## Step 1: ... steps omitted
The final answer is: $\boxed{\text{A1}}$. [/TRIAL]
[TRIAL] ## Step 1: ... steps omitted
The final answer is: $\boxed{\text{A2}}$. [/TRIAL]
[TRIAL] ## Step 1: ... steps omitted
The final answer is: $\boxed{\text{A1}}$. [/TRIAL]
[TRIAL] ## Step 1: ... steps omitted
The final answer is: $\boxed{\text{A1}}$. [/TRIAL]
The answer $\boxed{\text{A1}}$ has occurred three times, and is considered as a consensus.
The final answer is $\boxed{\text{A1}}$. I hope it is correct.

Non-Voting Response (ASV Case 2)

[TRIAL] ## Step 1: ... steps omitted
The final answer is: $\boxed{\text{A1}}$. [/TRIAL]
Terminated due to difficulty level.

Figure 4: Prompt templates. For $\mathcal{G}_\circ$, we use the SCoT prompt without including an additional [condition description] and generate a standard SCoT response. For $\mathcal{G}_+$, we simply insert the corresponding condition into the [condition description] placeholder to create a new prompt. In the case of SV, the SV condition is integrated into the prompt, and the model is asked to perform repeated trials to reach a consensus. The ASV prompt instructs the model to output either a voting response (case 1) or a non-voting response (case 2), with the decision made by the model itself.

For the description of training and testing details, we use LLaMA and LLaMA-b to denote the instruction-tuned and base versions of the LLaMA 3.1 8B models (Dubey et al., 2024), respectively. MATH refers specifically to the training split of the Hendrycks MATH dataset (Hendrycks et al., 2021b), while the 500-sample subset of the testing split is referred to as MATH500 (Lightman et al., 2023). SDPO stands for step-DPO (Lai et al., 2024) dataset, a curated step-annotated dataset from which we retain only the prompts and positive responses (ground truth solutions), excluding any step signals (see Appendix G for details). It is important to note that while we leverage their curated dataset, the original SDPO method is not relevant to this work. The SDPO dataset was chosen because its ground truth responses follow the SCoT format of LLaMA responses, making it convenient to run supervised fine-tuning (SFT) mixed with LLaMA samples.

Table 4: Summary of constructed datasets for different experimental purposes. $\mathbb{D}_{\text{SV}}$, $\mathbb{D}_{\text{ESSV}}$ and $\mathbb{D}_{\text{ASV}}$ uses the same set of prompts but different prompt/response templates. $\mathbb{Q}_{\text{SDPO}}$ and $\mathbb{A}^{\text{GOLDEN}}_{\text{SDPO}}$ are from Lai et al. (2024) with details deferred to Appendix G. ASV1 and ASV2 correspond to ASV case 1 and 2 (see Section B.1) respectively.

Set	$\mathcal{T}_q$	$\mathcal{T}_a$	$\mathcal{F}$	$\mathbb{Q}$	$\mathbb{A}$
$\mathbb{D}_{\text{SV}}$ $\mathbb{D}_{\text{ASV1}}$	SV ASV	SV ASV1	G	$\mathbb{Q}_{\text{MATH}}$	$\mathbb{A}^{\text{SAMPLE}}_{\text{MATH}}$
$\mathbb{D}_{\text{ASV2}}$ $\mathbb{D}_{\text{SCOT}}$	ASV SCoT	ASV2 SCoT	- -	$\mathbb{Q}_{\text{SDPO}}$	$\mathbb{A}^{\text{GOLDEN}}_{\text{SDPO}}$
$\mathbb{D}_{\text{RL}}$	ASV	-	-	$\mathbb{Q}_{\text{SDPO}}$	$\emptyset$

Table 5: Stopping conditions.

	stopping conditions
SV	(i) max 8 trials; (ii) if an answer occurs 3 times.
ASV	voting (case 1): (i) max 8 trials; (ii) if an answer occurs 3 times; non-voting (case 2): exact 1 trial.

Table 6: Prompt and response sources.

Set	Query-Response	Source
Training	$\mathbb{Q}_{\text{MATH}}$ & $\mathbb{A}^{\text{SAMPLE}}_{\text{MATH}}$ $\mathbb{Q}_{\text{SDPO}}$ & $\mathbb{A}^{\text{GOLDEN}}_{\text{SDPO}}$	MATH & LLaMA samples (Lai et al., 2024)
Testing	$\mathbb{Q}_{\text{MATH500}}$	MATH500

Table 7: Training pipelines. For Sec. B.2, we aim to create a demonstration experiment showing that with the same model (of roughly same math knowledge) SV can achieve reasonable performance-cost efficiency on par with MV. Sec. 5 further show we can optimize performance-cost efficiency through our IuB generalization of CGPO, where α in row 2.1 is a coefficient of $\mathbb{D}_{\text{ASV2}}$.

Exp.	Sec.	Type	Init. Ckpt.	Dataset	Purpose
1.1 1.2	Sec. B.2 Sec. 5	SFT SFT	LLaMA-b LLaMA	$\mathbb{D}_{\text{SV}} \cup \mathbb{D}_{\text{SCOT}}$	Allow model follow both SV and SCoT prompt.
2.1 2.2	Sec. 5	SFT RL	LLaMA Exp. 2.1	$\mathbb{D}_{\text{ASV1}} \cup \alpha\mathbb{D}_{\text{ASV2}}$ $\mathbb{D}_{\text{RL}}$	Follow the ASV instruction to let model decide vote or not. Optimize the capability of dynamic budget allocation.

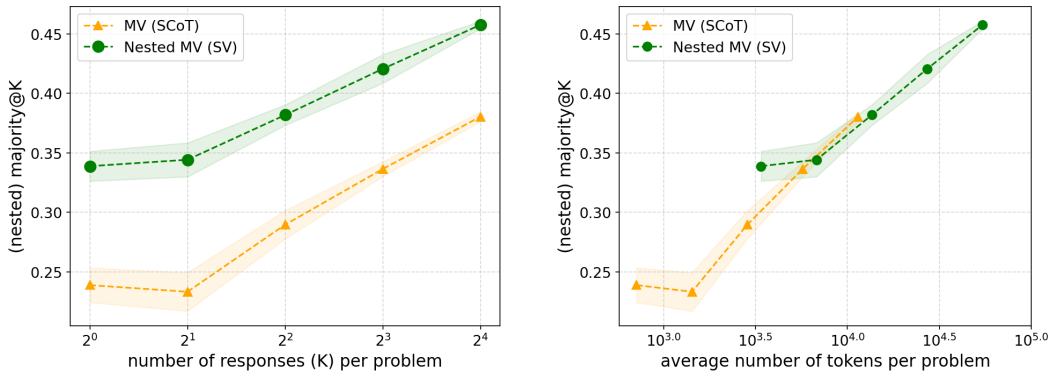

(a) (Nested) MV measured with number of responses

(b) (Nested) MV measured with number of tokens

Figure 5: SV tested on MATH500. MV stands for vanilla majority voting, aka self-consistency (Wang et al., 2022), with SCoT responses. Nested MV refers to majority voting with our (early-stopping) SV responses. It is "nested" as each SV response is already a voting, as shown in Figure 4. The SV method has "clear" gains when performance is measured with the number of responses. When measured with the number of tokens, SV aligns the performance-cost efficiency of vanilla MV. This is another indicator that one should worry about token efficiency when measuring reasoning performance.

Construction details. To be more specific, the naïve sequential voting baselines, as the "expensive" group $\mathcal{G}_+$, have increased inference costs by simply sequentially output multiple trials and find the sequential majority vote until stop condition met. In particular, the early-stopping sequential voting (SV) baseline is created to show that such naïve baseline could achieve performance gain, on par with vanilla majority voting (MV). The adaptive sequential voting (ASV) allows model to output both SCoT response $y_\circ$ and sequential voting response y_+, allowing us to further conduct the budget controll experiments in Section 5.

- Early Stopping Sequential Vote (SV): For a single response, model are allowed to output at most 8 trials, and conclude with majority of trials. In addition to the terminal condition of maximum 8 trials, model will early stop if an answer appears 3 times and this answer will be considered as the majority answer.
- Adaptive Sequential Vote (ASV): Model is allowed to choose either vote (case 1, i.e. y_+) or not (case 2, i.e. $y_\circ$). This baseline is created to further allow model-driven resource allocation. We later, in Section 5, show that one could optimize the ability of resource allocation with our IBPO.

Dataset. We define our construction of dataset as a product of a problem set $\mathbb{Q}$, format template of question $\mathcal{T}_q$ and answer $\mathcal{T}_a$, and a response set $\mathbb{A}$, subjected to some filtration $\mathcal{F}$. Formally, a dataset $\mathbb{D}$ is defined as: $\mathbb{D} := (\mathcal{F} \circ \mathcal{T}_q \circ \mathcal{T}_a)(\mathbb{Q} \times \mathbb{A})$, where $\mathcal{F}$ removes undesired question-answer pairs, such as incorrect responses when $\mathbb{A}$ are model generated; The templates $\mathcal{T}_q$ and $\mathcal{T}_a$ collectively transform each question-answer pair into a specific text format, as shown in Figure 4; Slightly abusing the notation, the Cartesian product $\mathbb{Q} \times \mathbb{A}$ is used to pair each response with its corresponding question, defined as: $\mathbb{Q} \times \mathbb{A} := \{(q_i, a_{ij}) : \forall i, j\}$.

Specifically, we summarize the datasets used in subsequent sections in Table 4. For instance, for SV training, we construct $\mathbb{D}_{\text{SV}}$ with question set $\mathbb{Q}_{\text{MATH}}$ from Hendrycks et al. (2021b) and LLaMA generated responses $\mathbb{A}_{\text{MATH}}^{\text{SAMPLE}}$ using the SV templates defined in Figure 4, subjected to data selection described in Appendix G.

Training pipelines. We summarize our training pipelines for our toy experiments in Section B.2 and our IuB experiments in Section 5. For instance, experiment 2.2 (Section 5) in Table 7 is the summary of our IBPO training, using dataset $\mathbb{D}_{\text{RL}}$ as constructed in Table 4 and initialized from ASV models from experiment 2.2. Further details of each training can be found in Appendix G and H.

B.2 Performance of Naïve Sequential Vote

We start by evaluating the performance of SV compared to vanilla MV, following the setup of Exp. 1.1 in Table 7. This toy experiment is designed to demonstrate: (i) SV scales approximately as well as MV, thereby qualifying it as an example of $\mathcal{G}_+$; and (ii) measuring performance based on the number of responses is inadequate, therefore we later measure performance relative to the number of tokens/trials in Section 5.

Metrics. The metrics we use are pass@k and majority@k, both of which are widely used in the literature (Hendrycks et al., 2021b; Wang et al., 2022). We occasionally refer to pass rate as pass@1. In both metrics, k specifically denotes the number of responses, regardless of the number of trials per response. Since our voting methods may involve multiple trials, we may use the average number of trials (as illustrated in Figure 2) on the x-axis for cost-aware comparisons. In addition, we evaluate "performance-cost" efficiency by comparing each method's scaling efficiency to that of MV, following the comparison in Snell et al. (2024).

As shown in Figure 5a, SV exhibits significant improvements—nearly 10%—in terms of majority@k when performance is measured by the number of responses. However, this improvement is misleading since each SV response effectively consists of multiple SCoT responses. Therefore, measuring performance with taking length into consideration provides a more reasonable assessment. As demonstrated in Figure 5b, SV's scaling performance aligns with that of vanilla MV, supporting its role as a suitable construction example for $\mathcal{G}_+$.

C SAMPLE RESPONSES

We show a couple of example responses of ASV-IuB-50%, the omitted prompt could be found in Figure 4.

Voting Example

Prompt omitted ...
Problem: Compute $\arcsin\left(-\frac{1}{2}\right)$. Express your answer in radians.
[TRIAL] ## Step 1: Recall the definition of arcsine The function $\arcsin x$ is the inverse of the sine function. It returns the angle whose sine is x.
Step 2: Use the unit circle to find the angle From the unit circle, we know that $\sin\left(-\frac{\pi}{3}\right) = -\frac{1}{2}$.
Step 3: Determine the value of $\arcsin\left(-\frac{1}{2}\right)$ Since $\sin\left(-\frac{\pi}{3}\right) = -\frac{1}{2}$, we have $\arcsin\left(-\frac{1}{2}\right) = -\frac{\pi}{3}$.
The final answer is: $\boxed{-\frac{\pi}{3}}$. [/TRIAL]

[TRIAL] ## Step 1: Recall the sine function values for common angles. The sine of $\frac{\pi}{3}$ is $\frac{\sqrt{3}}{2}$.
Step 2: Use the relationship between sine and arcsine. Given $\sin(\theta) = -\frac{1}{2}$, we are looking for $\arcsin\left(-\frac{1}{2}\right)$.
Step 3: Identify the angle whose sine is $-\frac{1}{2}$. From the unit circle or trigonometric identities, we know that $\sin\left(-\frac{\pi}{6}\right) = -\frac{1}{2}$.
Step 4: Express the answer in radians. Therefore, $\arcsin\left(-\frac{1}{2}\right) = -\frac{\pi}{6}$.
Therefore, the final answer is: $\boxed{-\frac{\pi}{6}}$ [/TRIAL]

[TRIAL] ## Step 1: Recall the sine function's relationship with the unit circle. The sine of an angle in a right triangle is the ratio of the length of the side opposite the angle to the length of the hypotenuse. For angles in the unit circle (a circle with radius 1), the sine of an angle is the y-coordinate of the point where the terminal side of the angle intersects the circle.
Step 2: Identify the angle with a sine of $-\frac{1}{2}$. From the unit circle, we know that $\sin\left(\frac{\pi}{3}\right) = \frac{1}{2}$. Since sine is negative in the third and fourth quadrants, and we are looking for an angle whose sine is $-\frac{1}{2}$, the angle must be in either the third or fourth quadrant.
Step 3: Determine the angle in the correct quadrant. Considering the unit circle, the reference angle for $\frac{\pi}{3}$ is $\frac{\pi}{3}$ itself. Since we are looking for an angle with a sine of $-\frac{1}{2}$, and knowing that sine is negative in the third and fourth quadrants, the angle we are looking for is in the fourth quadrant because $\sin\left(\frac{5\pi}{3}\right)$ would indeed be negative.
Step 4: Calculate the angle. The angle whose sine is $-\frac{1}{2}$ is $\frac{5\pi}{3}$.
Therefore, the final answer is: $\boxed{\frac{5\pi}{3}}$ [/TRIAL]

[TRIAL] ## Step 1: Recall the definition of arcsine The function $\arcsin x$ is the inverse of the sine function. It returns the angle whose sine is x.
Step 2: Use the sine function to find the angle We want to find the angle whose sine is $-\frac{1}{2}$. We can use the sine function to find this angle.
Step 3: Recall common angles and their sines From the unit circle or trigonometric identities, we know that $\sin\left(\frac{\pi}{6}\right) = \frac{1}{2}$. Since sine is an odd function, $\sin\left(-\frac{\pi}{6}\right) = -\frac{1}{2}$.
Step 4: Determine the angle Therefore, the angle whose sine is $-\frac{1}{2}$ is $-\frac{\pi}{6}$.
Therefore, the final answer is: $\boxed{-\frac{\pi}{6}}$ [/TRIAL]

[TRIAL] ## Step 1: Recall the sine function's values for common angles. The sine function has well-known values for certain angles. Specifically, $\sin\left(\frac{\pi}{6}\right) = \frac{1}{2}$.
Step 2: Use the symmetry and periodicity of the sine function. Given that $\sin\left(\frac{\pi}{6}\right) = \frac{1}{2}$, and knowing that sine is an odd function, we have $\sin\left(-\frac{\pi}{6}\right) = -\frac{1}{2}$. This step utilizes the property of odd functions where $f(-x) = -f(x)$.
Step 3: Solve for $\arcsin\left(-\frac{1}{2}\right)$. Given that $\sin\left(-\frac{\pi}{6}\right) = -\frac{1}{2}$, the angle whose sine is $-\frac{1}{2}$ is $-\frac{\pi}{6}$. This is because the inverse sine function, $\arcsin$, returns the angle whose sine is a given value.
Therefore, the final answer is: $\boxed{-\frac{\pi}{6}}$ [/TRIAL]

The answer $\boxed{-\frac{\pi}{6}}$ has occured three times and is considered as a consensus. The final answer is $\boxed{-\frac{\pi}{6}}$.
I hope it is correct.

Non-voting Example

Prompt omitted ...

Problem: If $f(x) = \frac{3x-2}{x-2}$, what is the value of $f(-2) + f(-1) + f(0)$? Express your answer as a common fraction.

[TRIAL] ## Step 1: Substitute $x = -2$ into the function $f(x)$. To find $f(-2)$, substitute $x = -2$ into the function:

$$f(-2) = \frac{3(-2) - 2}{-2 - 2} = \frac{-6 - 2}{-4} = \frac{-8}{-4} = 2.$$

Step 2: Substitute $x = -1$ into the function $f(x)$. To find $f(-1)$, substitute $x = -1$ into the function:

$$f(-1) = \frac{3(-1) - 2}{-1 - 2} = \frac{-3 - 2}{-3} = \frac{-5}{-3} = \frac{5}{3}.$$

Step 3: Substitute $x = 0$ into the function $f(x)$. To find $f(0)$, substitute $x = 0$ into the function:

$$f(0) = \frac{3(0) - 2}{0 - 2} = \frac{0 - 2}{-2} = \frac{-2}{-2} = 1.$$

Step 4: Sum the values of $f(-2)$, $f(-1)$, and $f(0)$. Sum the calculated values:

$$f(-2) + f(-1) + f(0) = 2 + \frac{5}{3} + 1.$$

Step 5: Simplify the sum to express it as a common fraction. To combine the terms into a common fraction, convert the whole numbers to fractions with a common denominator:

$$2 + \frac{5}{3} + 1 = \frac{6}{3} + \frac{5}{3} + \frac{3}{3} = \frac{6 + 5 + 3}{3} = \frac{14}{3}.$$

Therefore, the value of $f(-2) + f(-1) + f(0)$ is $\frac{14}{3}$.

Therefore, the final answer is: $\boxed{\frac{14}{3}}$ [/TRIAL]

Terminated due to difficulty level.

D INTEGER LINEAR PROGRAM SOLVING

We use SciPy MILP solver, available here, to solve an integer LP every iter. Figure 1 is a Pythonic pseudo-code. And the wall-time consumed could be found in Figure 6. As the problem size is small, so the computational overhead is negligible.

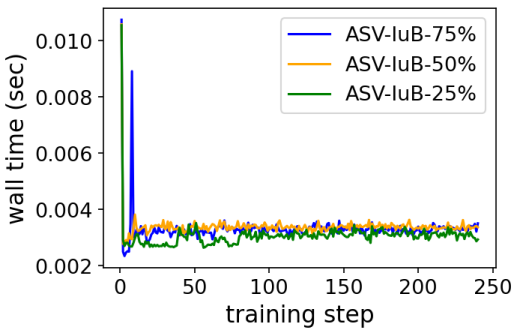

Figure 6: Wall time (averaged across ranks) spent by solver in seconds.

```python
import numpy as np
from scipy.optimize import milp, LinearConstraint, Bounds

def solve_iub(acceptance, is_vote, budget):
    """ solves a Inference under Budget (IuB) problem. Parameters:
    - acceptance: an n x m array where each element is 1 if accepted, 0 otherwise.
    - is_vote: an n x m array indicating whether response is voting (1) or non-voting (0).
    - budget: the fractional budget (q+) constraint for the problem. """
    n, m = acceptance.shape
    # calculate pass rates for vote-based and non-vote-based responses
    vote_pass_rate = np.mean(acceptance * is_vote, axis=1, keepdims=True)
    sample_pass_rate = np.mean(acceptance * (1 - is_vote), axis=1, keepdims=True)
    margin = vote_pass_rate - sample_pass_rate  # (n, 1)
    # flattern acceptance and vote indicator, tile the margin
    acceptance = np.reshape(acceptance, -1)             # (n x m, )
    is_vote = np.reshape(is_vote, -1)                   # (n x m, )
    margin = np.reshape(np.tile(margin, [1, m]), -1)    # (n x m, )

    # define the objective function coefficients
    c = -1 * margin * is_vote + margin * (1 - is_vote)
    # acceptance constraints: ensure each prompt meets acceptance criteria
    A_acceptance = np.eye(len(acceptance))
    b_acceptance = acceptance
    # one response per problem constraint (BoN)
    A_problem = np.zeros((n, n * m))
    for i in range(n):
        A_problem[i, i * m:(i + 1) * m] = 1
    b_problem = np.ones(n)
    # voting responses budget constraint
    A_vote_budget = np.where(is_vote == 1, 1, 0).reshape(1, -1)
    vote_budget = np.round(budget * len(acceptance))

    # combine all constraints into a single matrix
    A = np.vstack([A_acceptance, A_problem, A_vote_budget])
    b_lower = -np.inf * np.ones(A.shape[0])  # lower bounds for constraints
    b_upper = np.hstack([b_acceptance, b_problem, vote_budget])  # upper bounds
    # solve the MILP problem using the defined objective and constraints
    result = milp(c, integrality=np.ones(len(c)), bounds=Bounds(0, 1),
                  constraints=LinearConstraint(A, b_lower, b_upper))
    return result
```

Listing 1: Pythonic code snippet for solving IuB with SciPy: Note that this is for demonstration purposes, and error-free execution is not guaranteed, due to omitted corner cases.

E BATCH ACCUMULATION

This is a batch accumulation implementation of Algorithm 1. For brevity, we use OPT_{IUB} as an example. One could increase the optimization problem size of $n \times m$ to $(n \cdot k_b) \times (m \cdot k_r)$ using Algorithm 2, where superscripts indicate matrix shape, left subscripts denote accumulation indices (distinguishing them from element indices).

Algorithm 2 IBPO with Sample Accumulation

Require: prompt set $\mathbb{D}$, batch size n, num of responses m, init policy $\pi_0 = \pi_{\text{ref}}$, num of iters T, budgets q_+

for $t = 1, \ldots, T$ **do**
  for $i = 1, \ldots, k_b$ **do**
    prompt sampling: ${}_i\mathbf{X}^n \sim \mu_{\mathbb{D}}$
    for $j = 1, \ldots, k_r$ **do**
      response generation: ${}_{ij}\mathbf{Y}^{n\times m} \sim \pi_{\theta_t}({}_i\mathbf{X})$
    end for
  end for
  prompt accumulation: $\tilde{\mathbf{X}}^{(n\cdot k_b)} = [{}_1\mathbf{X}, {}_2\mathbf{X}, \cdots, {}_{k_b}\mathbf{X}]$
  response accumulation: $\tilde{\mathbf{Y}}^{(n\cdot k_b)\times(m\cdot k_r)} = [{}_{11}\mathbf{Y}, {}_{12}\mathbf{Y}, \cdots, {}_{1k_r}\mathbf{Y}; \cdots; {}_{k_b1}\mathbf{Y}, {}_{k_b2}\mathbf{Y}, \cdots, {}_{k_bk_r}\mathbf{Y}]$
  evaluate correctness and **empirical KL**: $\mathbf{R}_{\text{match}} = r_{\text{match}}(\tilde{\mathbf{X}}, \tilde{\mathbf{Y}})$ and $\hat{\mathbf{KL}} = \hat{\mathbb{KL}}(\tilde{\mathbf{Y}}; \tilde{\mathbf{X}}, \pi_{\text{ref}})$
  margin maximization: $\hat{\pi}^\star_{\tilde{\mathbf{X}},\tilde{\mathbf{Y}}} \in \text{OPT}_{\text{IUB}}(\tilde{\mathbf{X}}, \tilde{\mathbf{Y}}, \mathbf{R}_{\text{match}}, \hat{\mathbf{KL}}, q_+)$ as defined in Eq. (8)
  gradient update: with $-\sum_{i=1}^{n\cdot k_b}\sum_{j=1}^{m\cdot k_r} \hat{\pi}^\star_{\tilde{\mathbf{X}},\tilde{\mathbf{Y}}}(y_{ij}|x_i) \frac{\partial}{\partial\theta} \log \pi_\theta(y_{ij}|x_i)\big|_{\theta=\theta_t}$
end for

F TRAINING CURVES & FURTHER DISCUSSIONS

Budgets constraints. In Section 5, we show that the constraints hold exactly on the training set, for responses that are correct. Figure 7b further shows the ratio of voting responses for all online samples. It's clear that the constraints also hold.

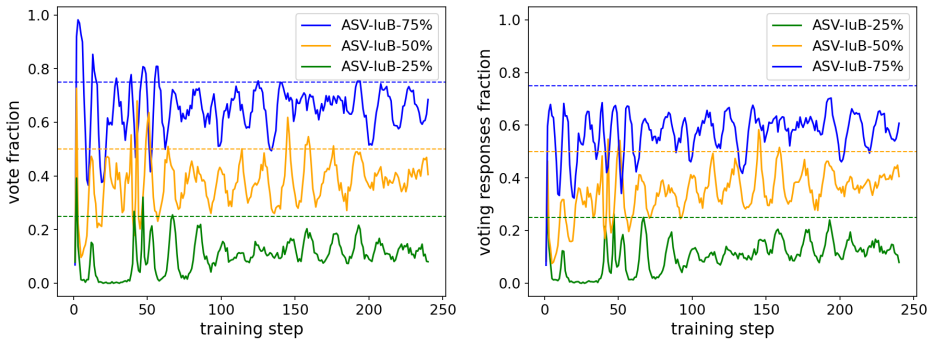

(a) Voting ratio of correct responses (training set) (b) Voting ratio of all responses (training set)

Figure 7: Voting response ratio versus training steps. Dashed line denotes the budget q_+. On the training set, IuB formulation follows the budget constraints almost exactly for both: (a) correct responses; (b) all responses.

CGPO on $\mathbb{D}_{\text{RL}}$ w/ LLaMA. To further understand the results we presented in Section 5 is benfit from our budget-aware formulation or from the prompt set of Lai et al. (2024). We further run CGPO with open-sourced LLaMA model and the SDPO dataset in the SCoT format. Figure 8 compares the training dynamics of CGPO with LLaMA versus our ASU-IuB-q_+ experiments. In general, the SDPO prompt set does not provide much additional knowledge as suggested by the OSS w/ vanilla CGPO experiment, but ASV-IuB-q_+ experiments are able to achieve noticable gain.

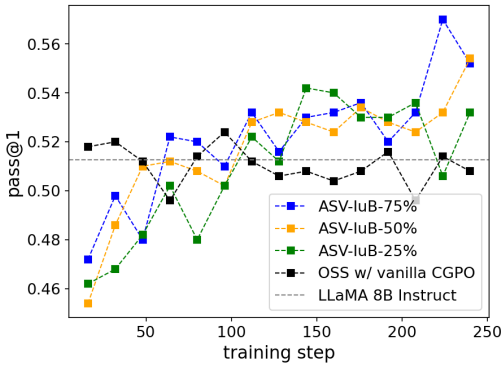

Figure 8: Training curves: each point corresponds an evaluation of MATH500 test set, and dashed line is the pass@1 of LLaMA 8B Instruct.

Controlled setting. Our experiment setting is minimal: we do not use reward models; we use only an 8B model to generate any set of sampled responses, $\mathbb{A}^{\text{SAMPLE}}$. Our RL training set, $\mathbb{D}_{\text{RL}}$, contains only 10k prompts, leaving the setting quite controlled and providing room for improvement through engineering efforts.

Limitations. Our work is limited in its choice of RL algorithms and applications. While it should be straightforward to apply our framework to different RL frameworks, additional effort is required to derive an optimization problem for different application tasks. Future work may include extending our constrained policy optimization framework to a broader range of LLM applications or scaling up our experiments.

G Data Construction

We elaborate on the details of $\mathbb{Q}_{\text{SDPO}}$, $\mathbb{A}^{\text{GOLDEN}}_{\text{SDPO}}$, $\mathbb{Q}_{\text{MATH}}$, $\mathbb{A}^{\text{SAMPLE}}_{\text{MATH}}$, and the filteration function $\mathcal{F}$.

SDPO dataset. Lai et al. (2024) create a dataset (see their Section 3.2) contains 10,795 step-wise preference pairs, where the winning response is a correct solution, the losing response is incorrect starting from certain step. For our purpose of SFT and RL training, we do not need losing responses, hence we create $\mathbb{A}^{\text{GOLDEN}}_{\text{SDPO}}$ with only wining (correct) responses. The step-formatted response (see an example below) is the reason we choose the dataset from Lai et al. (2024), as it adhere the SCoT format of LLaMA models. Therefore, one do not need to worry about potential format changes.

SDPO question-response example

Problem: Sides of a rectangular park are in the ratio 3: 2 and its area is 3750 sq m, the cost of fencing it at 40 ps per meter is?
Step 1: Let's assume the sides of the rectangle are $3x$ and $2x$. The area of the rectangle is the product of its sides, so we have $3x \cdot 2x = 6x^2 = 3750$. Solving for x, we get $x^2 = \frac{3750}{6} = 625$, so $x = \sqrt{625} = 25$.
Step 2: So the sides of the rectangle are $3x = 3 \cdot 25 = 75$ meters and $2x = 2 \cdot 25 = 50$ meters.
Step 3: The perimeter of the rectangle is $2 \times (75 + 50) = 2 \times 125 = 250$ meters.
Step 4: The cost of fencing is 40 paise per meter, so the total cost of fencing is $250 \times 40 = 10000$ paise. Since 1 rupee is equal to 100 paise, the cost in rupees is $\frac{10000}{100} = 100$ rupees.
Therefore, the final answer is: $\boxed{100}$

SV dataset for MATH. We also created datasets, $\mathbb{D}_{\text{SV}}$ and $\mathbb{D}_{\text{ASV1}}$, for SFT so that a model could follow the SV instructions. We take $\mathbb{D}_{\text{SV}}$ as an example and $\mathbb{D}_{\text{ASV1}}$ could be created similarly. To do so, we first generate 32 responses per prompt for the entire MATH training split with a temperature of 1.2 and top-p of 0.9. We then apply our SV templates $\mathcal{T}_q$ and $\mathcal{T}_a$ to create corresponding SV question and answer pairs. The procedure of creating a SV response is given by Algorithm 3. While we have include an example of SV responses in Figure 9, we make it more concrete the SV response template below,

SV template: $\mathcal{T}_a(A_1, \cdots, A_k,$ final answer) (if consensus found)

[TRIAL] $\{A_1\}$ [/TRIAL]
[TRIAL] $\{A_2\}$ [/TRIAL]
$\cdots$
[TRIAL] $\{A_k\}$ [/TRIAL]
The answer $\boxed{\text{final answer}}$ has occurred three times, and is considered as a consensus.
The final answer is $\boxed{\text{final answer}}$. I hope it is correct.

SV template: $\mathcal{T}_a(A_1, \cdots, A_8,$ final answer) (if no consensus found)

[TRIAL] $\{A_1\}$ [/TRIAL]
[TRIAL] $\{A_2\}$ [/TRIAL]
$\cdots$
[TRIAL] $\{A_8\}$ [/TRIAL]
Maximum trials reached but no consensus found due to a tie; the most plausible answer is $\boxed{\text{final answer}}$.
The final answer is $\boxed{\text{final answer}}$. I hope it is correct.

Figure 9: SV response templates. Left: suppose a consensus is found at k-th answer; Right: no consensus found. Note the subscript i of A_i only denotes index of answer, A_i and A_j could still have same final answer for $i \neq j$.

Algorithm 3 Creating SV Response for SFT .

Require: template $\mathcal{T}_q$, $\mathcal{T}_a$, a problem Q, a set of shuffled responses $\{A_i : i = 1, 2, \cdots, K\}$
create prompt: $\mathcal{T}_q(Q)$ replace problem placeholder with Q
responses = []; final_answer = [INVALID_ANSWER]; found = False
for $i = 1, 2, \cdots, K$ **do**
  responses.append(A_i)
  majority = find_majority(responses)
  majority_count = count_majority(responses, majority)
  if majority_count == 3 **then**
    found = True; final_answer = majority; break
  end if
end for
if found == False **and** responses contain correct solution **then**
  final_answer = random pick a correct solution
end if
create SV response: $\mathcal{T}_a$(responses, final_answer)

We then apply some filtration $\mathcal{F}$ to the created dataset. We remove SV responses whose final answers are incorrect. From the remaining set, we sub-sample 500 question-response pairs. These pairs are selected from problems that have between 4 and 8 distinct answers out of 32 samples, ensuring that we construct sequential responses with a diverse trials. The distribution of trial counts and distinct answer counts are shown in Figure 10. It can be observed that the filtered data is diversely distributed.

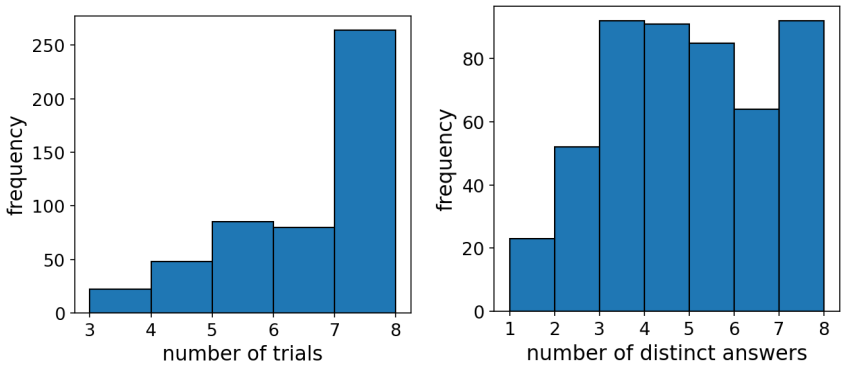

(a) Distribution of number of trials per response

(b) Distribution of number of distinct answers

Figure 10: The distribution of filtered prompt-responses subset, which suggests that the construct data is generally diversely distributed.

H HYPERPARAMETERS

We list the hyperparameters used for experiments setup 1.2, 2.1, 2.2, as described in Table 7. And we conduct our experiments with NVIDIA-A100-80Gs. (Please refer to Xu et al. (2024b) for the definition of some RL-specific hyper-parameters.)

Table 8: Hyperparameters for Experiment setups 1.2, 2.1, and 2.2

Hyperparameter	**Setup 1.2**	**Setup 2.1**	**Setup 2.2**
prompt size	11295	11295	10795
number of nodes	4	4	8
learning rate	1e-6	1e-6	5e-7
batch size (per node)	8	16	4
num of steps	1024	2048	240
optimizer	AdamW	AdamW	AdamW
scheduler	constant	constant	constant
packing	yes	yes	-
max sequence length	32768	32768	6144
gradient accumulation	1	2	1
RL-specific params			
num generation per prompt			8
max generation length			4096
temperature			1.0
top-p			0.9
KL-threashold			1024
batch accumulation k_b			4
response accumulation k_r			1